Spring 2017

A Geophysical Analysis of the Great Falls Tectonic Zone and the Surrounding Area, Montana USA

Travis Lane Fultz

A GEOPHYSICAL ANALYSIS OF THE GREAT FALLS TECTONIC ZONE AND THE SURROUNDING AREA, MONTANA USA

A Masters Thesis

Presented to

The Graduate College of

Missouri State University

In Partial Fulfillment

Of the Requirements for the Degree

Master of Science, Geospatial Science in Geography Geology and Planning

By

Travis L. Fultz

May 2017

A GEOPHYSICAL ANALYSIS OF THE GREAT FALLS TECTONIC ZONE AND THE SURROUNDING AREA, MONTANA USA

Geography, Geology and Planning

Missouri State University, May 2017

Master of Science

Travis L. Fultz

ABSTRACT

The Great Falls Tectonic Zone (GFTZ) is a northeast trending zone of high angle faults and lineaments extending from northeastern Idaho into Saskatchewan, Canada. The GFTZ is believed to have facilitated the collision between the Archean Wyoming and Hearne cratons. Previous geophysical studies have analyzed seismic refraction data across the boundary between the Paleoproterozoic GFTZ and Archean Wyoming Craton (WC), this indicated the lower crustal layer thickens as it dips beneath the boundary towards the WC. In this study, three 2 dimensional (2D) gravity models that crossed the central region of the GFTZ were produced using constraints from existing geologic and geophysical studies. The construction of a complete Bouguer gravity anomaly map, regional and residual (band-pass filtered) gravity and magnetic maps, as well as the generation of 2D magnetotelluric electrical resistivity profiles greatly aided in the interpretation of areas of interest. Coupled with the newly developed maps, the models provide otherwise unavailable constraints on the extent and geometries of the GFTZ/WC boundary region. Additional geophysical analysis of these features may substantiate the findings and help redefine the subsurface extent of the GFTZ/WC boundary. Low resistivity values in the upper mantle may be related to release water formed during subduction of cratonic material during the Paleoproterozoic.

KEYWORDS: Great Falls Tectonic Zone, gravity, magnetics, magnetotellurics, Wyoming craton, paleoproterozoic tectonics

This abstract is approved as to form and content

_____

Dr. Kevin Mickus
Chairperson, Advisory Committee
Missouri State University

A Geophysical Analysis of The Great Falls Tectonic Zone

And The Surrounding Area, Montana USA

By

Travis Lane Fultz

A Masters Thesis
Submitted to the Graduate College
Of Missouri State University
In Partial Fulfillment of the Requirements
For the Degree of Master of Science, Geology, Geography, and Planning

May 2017

Approved:

_____
Dr. Kevin Mickus

_____
Dr. Douglas Gouzie

_____
Dr. Melida Gutierrez

_____
Dr. Julie Masterson, Dean, Graduate College

ACKNOWLEDGEMENTS

I would like to acknowledge and thank my committee members, Dr. Douglas Gouzie and Dr. Melida Gutierrez and especially my primary advisor Dr. Kevin Mickus, for the support and direction they have continually provided. I would like to acknowledge the Graduate College for funding assistance that helped make the field research possible and faculty of the Department of Geography, Geology and Planning for providing an excellent environment to learn and achieve. I would also like to give a special thanks to Mr. Bob Schellhorn for his generous donation in making this project a reality.

Finally, I would like to thank the following people for their personal support and encouragement: Drew Thomas, Johnny Bertalott, Mark Larson, Eva and Tayler Fultz, my mother and father, and the many others too numerous to mention here.

TABLE OF CONTENTS

LIST OF FIGURES

1.0 INTRODUCTION

1.10 Setting

It is generally accepted that the geological age of the Earth is approximately 4.60 billion years old (Ga). During that time, the continents have undergone several different configurations. Roughly 200 million years ago the supercontinent Pangaea began to break apart. By approximately 90 million years ago, the continents of North and South America began separating from Pangaea forming what is now the Atlantic Ocean region. The oldest tectonic element within the North American continent, the Wyoming Province, is within the northwestern region of the United States and includes regions in Wyoming and Montana. The Archean provinces within Wyoming, Montana, and southern Alberta have endured periods of Proterozoic rifting (2.45-2.10 Mya.), collisional amalgamation (1.96-1.83 Mya.), and volcanic pulses (~1.9-1.77 Mya.), along with intense deformational events during the Laramide and Sevier orogenies (Whitmeyer and Karlstrom, 2007).

A key element to Laurentia's assembly includes the incorporation of the Archean provinces of Wyoming, Medicine Hat Block, and Hearne (Chamberlain et. al. 2003; Whitmeyer and Karlstrom, 2007). The incorporation of these cratonic blocks into the core of Laurentia has provided researchers with an extraordinary tapestry of some of the most interesting and complex geology within the North American continent.

The Great Falls Tectonic Zone (GFTZ) is a northeast-trending zone of faults and lineaments extending from Saskatchewan into northeastern Idaho (Boerner et. al. 1998). The GFTZ is an important geologic feature since it facilitates the interaction of the Wyoming and Medicine Hat Block cratonic provinces; however, the true nature of the GFTZ and the Wyoming Province remains unknown due to Phanerozoic sediments

completely covering the region (Mueller et al. 2002). The relationship between the Proterozoic-aged GFTZ and the surrounding tectonic provinces are illustrated in Figure 1. On the western edge of the cratons lies the Belt Basin, which includes both Archean and Proterozoic-aged rocks (Mueller and Frost, 2006), with the Paleoproterozoic Trans-Hudson (Dakota) Orogen on its eastern border (Foster et al. 2006).

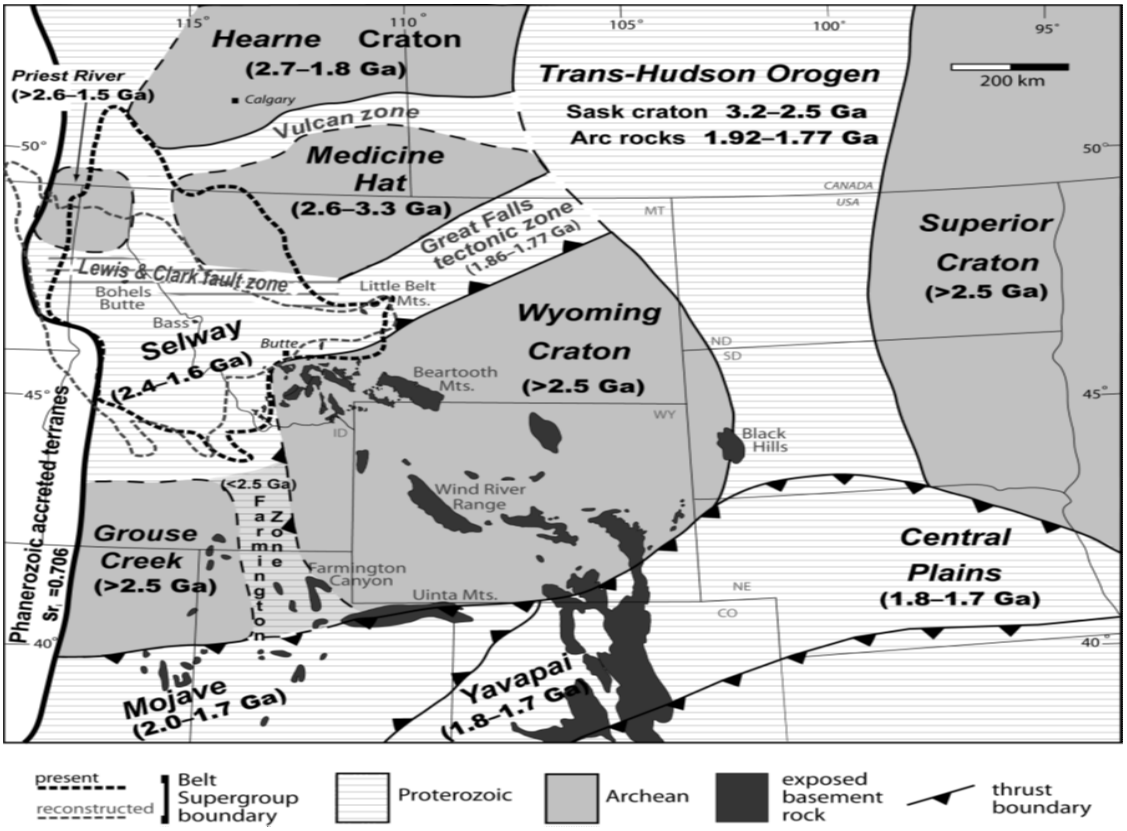

Figure 1. Archean and Proterozoic provinces of the study area which illustrates the relationship between the GFTZ and the surrounding features, modified from Foster et al. (2006)

Current theories regarding the origin of the GFTZ include: 1) it marks the Paleoproterozoic collision between the Wyoming, Medicine Hat Block, and Hearne provinces (Whitmeyer and Karlstrom, 2007), 2) it is a reactivated Archean intracratonal

shear zone (Boerner et al. 1998), and 3) it is another type of geologic feature, such as a strike slip region or a suture zone between the Wyoming and Hearne provinces (Whitmeyer and Karlstrom, 2007).

1.20 Previous Studies

The limited information that is known about the region has been acquired through commercial drilling exploration, limited regional geophysical experiments and scattered Archean and Proterozoic outcrops within Montana and northern Wyoming (Chamberlain et al. 2003). Figure 2 shows the limited outcrops within the study due to the few Laramide-aged uplifts.

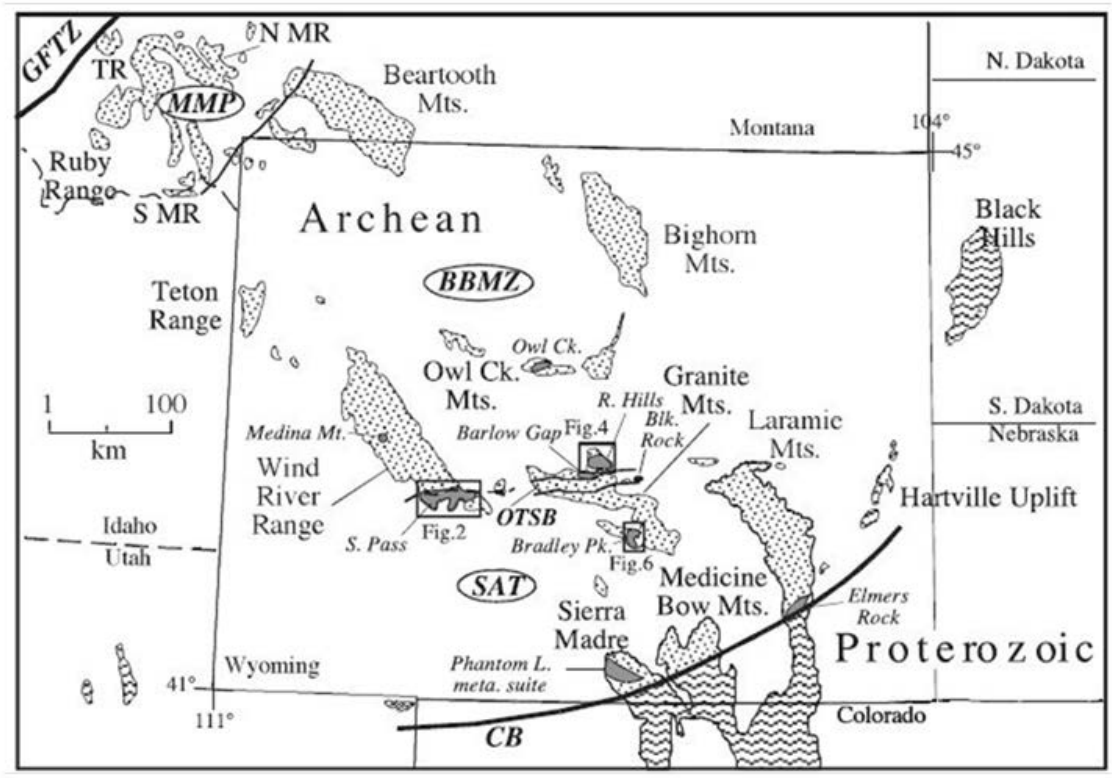

Figure 2. Location of Archean rocks in the study area exposed by Laramide deformation. Modified from Chamberlain et al. (2003).

1.30 Previous Seismic and Magnetotelluric Studies

The regional geophysical studies conducted in the study area have included various seismic reflection and refraction studies (Gorman et al. 2000; Clowes et al. 2002), gravity studies of the GFTZ and magnetotellurics (MT) studies in the Trans Hudson region (Boerner et al. 1998; Mickus, 2007).

There are two main, regional seismic refraction experiments that provide information of the crust and mantle structures within the Medicine Hat Block, GFTZ, and northern Wyoming Province regions. The Southern Alberta Refraction Experiment (SAREX) was carried out in conjunction with the Deep Probe seismic experiment (Gorman et al. 2000; Clowes et al. 2002), (Figures 3 and 4). These studies determined the velocity structures of the crust and upper mantle of the Archean regions as well as Phanerozoic altered regions of the western North American continent (Gorman et al. 2000; Clowes et al. 2002).

The SAREX experiment was recorded over the Western Canada Sedimentary Basin (WCSB) which extends into northeastern Montana (Clowes et al. 2002). There are approximately 2000m of sedimentary rocks overlying the crystalline basement within the WCSB which considerably affects seismic wave arrival times. The final velocity model from the SAREX experiment determined upper crystalline crustal velocities of 6.0-6.5 km/s that remained consistent to depths of approximately 20 km (Figure 5). These upper crustal velocities also remained consistent laterally along the profile, with the exception of a remarkable trough-like feature at depths between 20-30 km in the northern half of the profile. These trough-like features range in velocity from 6.5-7.0 km/s and are

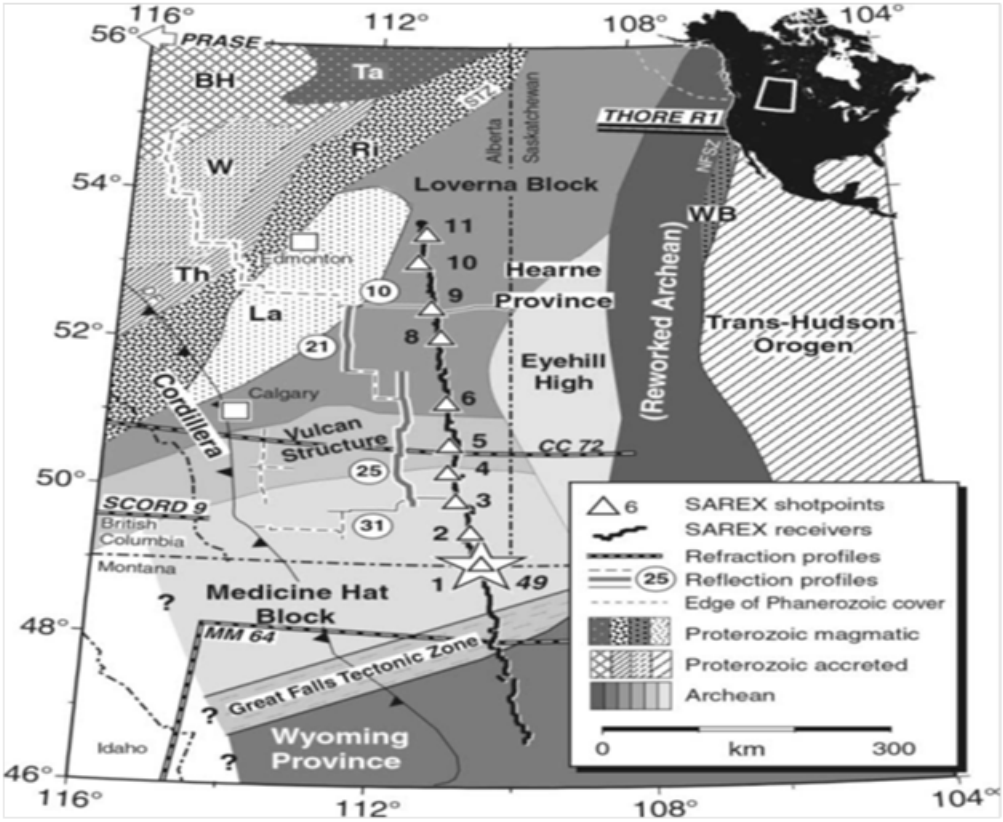

Figure 3. Location of the SAREX and Deep Probe experiments overlain on the tectonic province of the region. The star labeled 49 is SAREX 1 & Deep probe shot 49. Numbered circles are reflection profiles compared directly to SAREX results. The triangles represent SAREX shot points. Modified from Clowes et al. (2002).

interpreted to be deformed lower crustal material. On the southern end of the profile, beginning just north of the USA-Canada border, there is a higher velocity layer extending at least 300km southward under the Wyoming Province with velocities of 7.5 km/s. This high velocity layer, labeled LCL in Figure 5, is interpreted to be a Proterozoic ultramafic underplated body. Consequently, the WP extends to a depth of approximately 57-60 km with the addition of the ultramafic underplating, which on average is 20km thicker than the global crustal thickness beneath other cratonic features (Gorman et al. 2002).

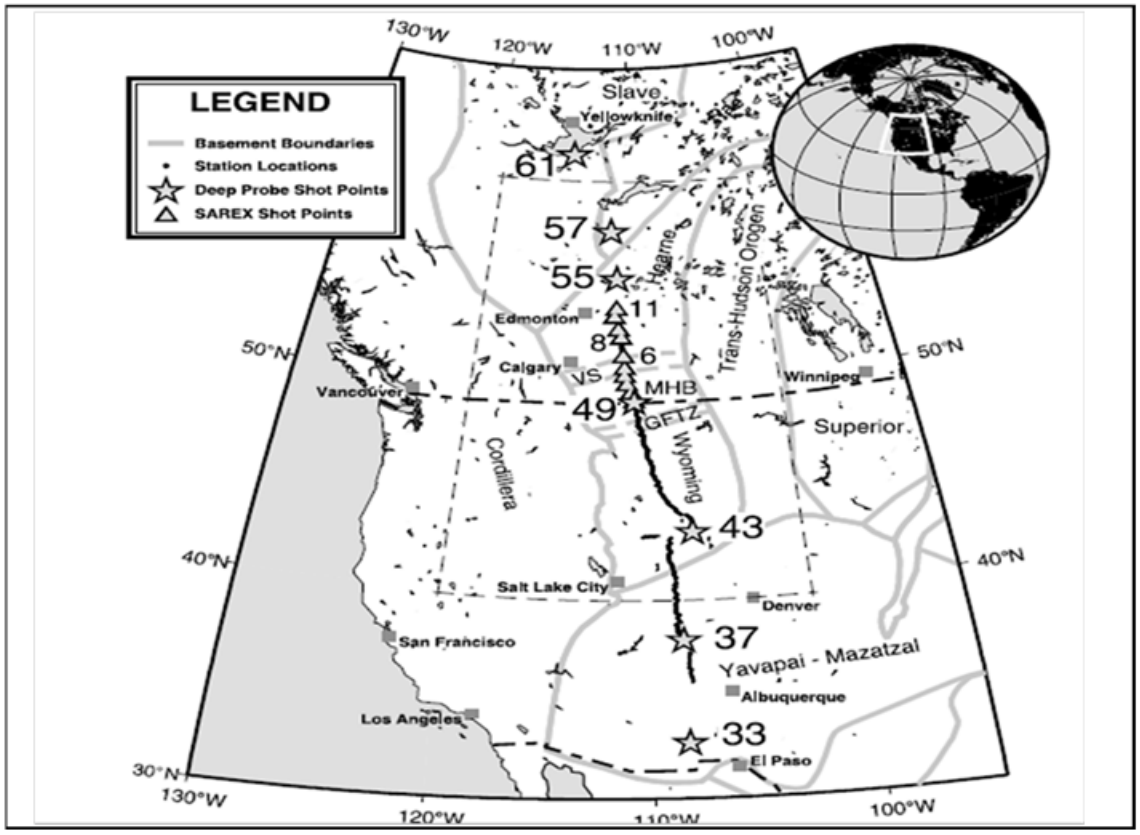

Figure 4. Locations of SAREX and Deep Probe shot locations. Single digit numbered triangles represent SAREX shot points, double digit numbered stars represent Deep Probe shot points. Medicine Hat Block-MHB; Vulcan Structure-VS; Great Falls Tectonic Zone-GFTZ. Grey lines indicate regional tectonic boundaries. Modified from Gorman et al. (2000).

The Deep Probe experiment, (Gorman et al. 2000) was carried out in conjunction with the SAREX experiment. The Deep Probe experiment was a state of the art seismic refraction-wide angle reflection (R/WAR) experiment. While there have been other R/WAR experiments, only those by Iyer et al. (1969), Thybo and Perchuc (1997), Németh and Hajnal (1998) have extended long enough to provide velocity sections for the entire lithospheric mantle of the continents. The final velocity model from the Deep

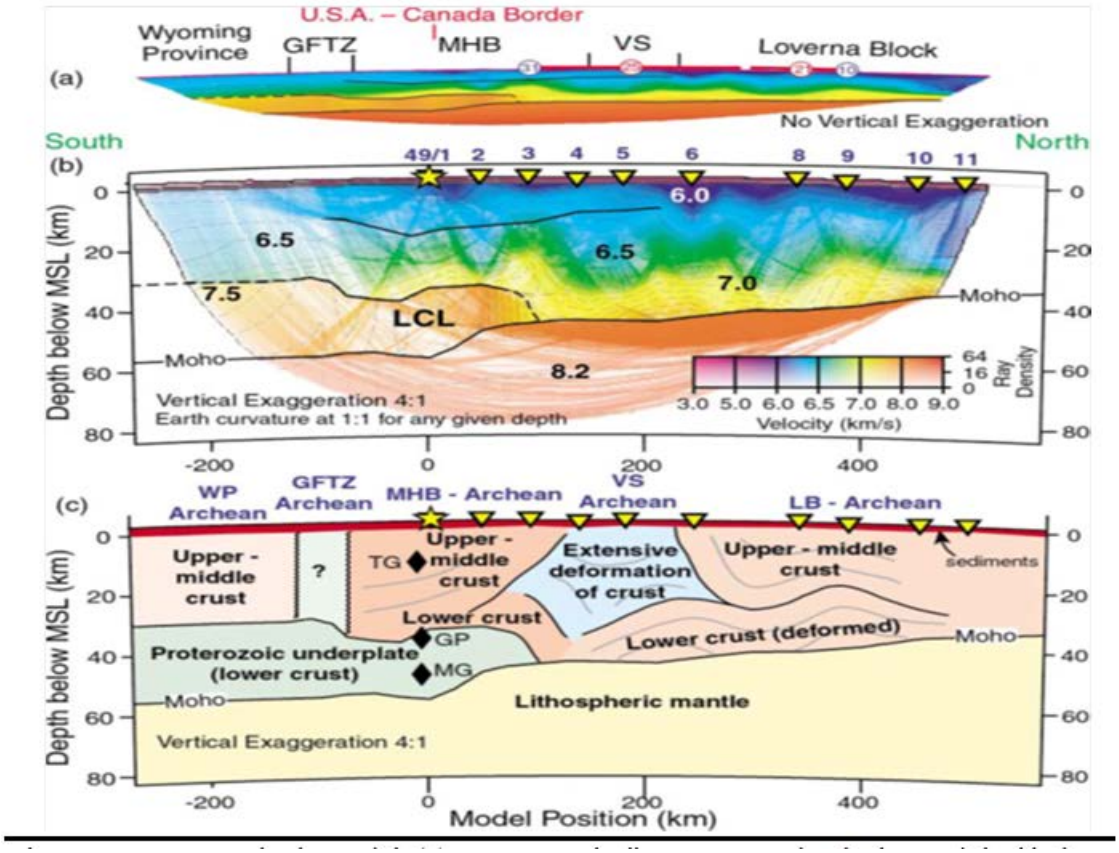

Figure 5. SAREX seismic model. (a) 1:1 nonvertically exaggerated velocity model with the various colors representing different velocities. (b) 4:1 vertically exaggerated velocity model showing ray trace paths. Numbers represent ray travel times in km/s. (c) geological representation of their velocity model based on both SAREX and Deep Probe data. Lower crustal layer-; black diamonds are xenolith samples; tonalite gneiss-TG garnet paragneiss-GP; mafic granulite-MG. Numbered circles, triangles, and stars represent various shot locations. Modified from Clowes et al.(2002).

Probe experiment is shown in Figure 6. The Deep Probe and SAREX models appear comparable at first glance; however, there are several variations and additional conclusions due to both processing methods and added Deep Probe shot data points (Clowes et al. 2002, Gorman et al. 2000).

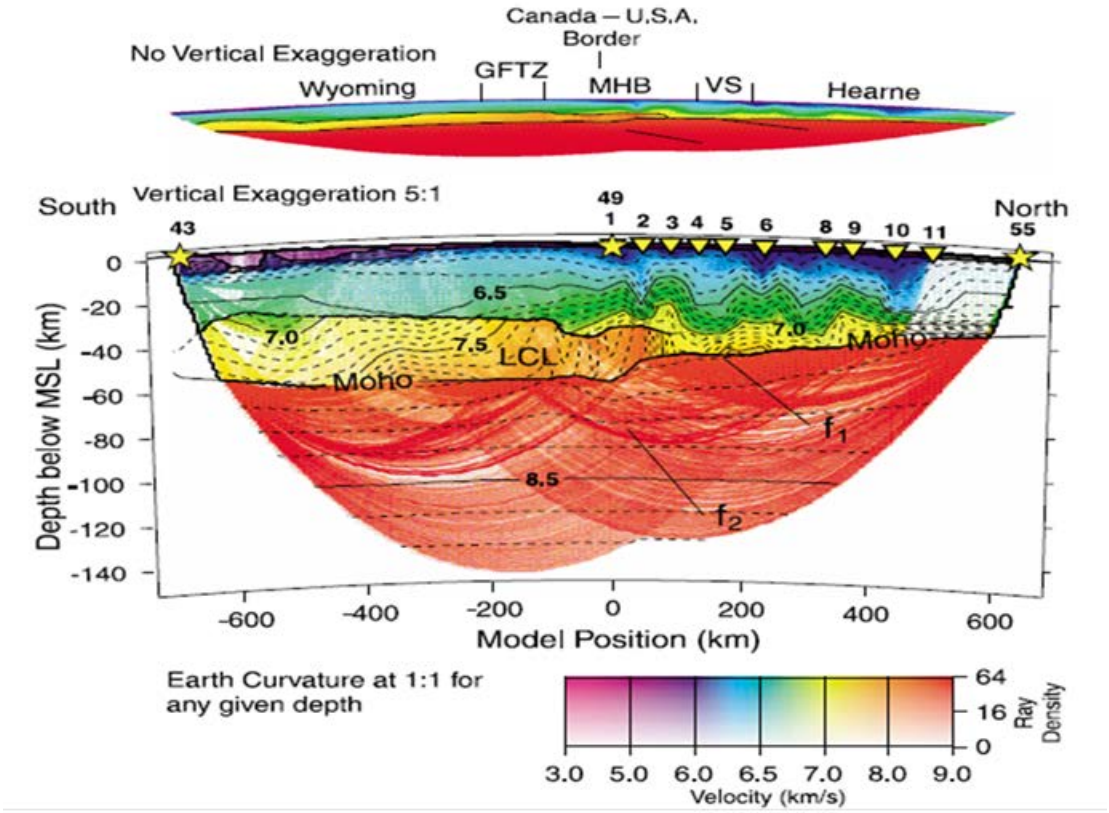

Figure 6. Final seismic model of the Deep Probe experiment. Stars and triangles represent shot points. Lower crustal layer-LCL; f1 and f2 represent floating mantle reflectors; Vulcan structure-VS; Medicine Hat Block-MHB; Great Falls Tectonic Zone-GFTZ. Modified from Gorman et al. (2000).

Like the SAREX model, the Deep Probe model depicts four basic rock layers; an upper and lower crust, an underplated layer, and finally the mantle layer. Seismic velocities between both models remain consistent, although Gorman et al. (2000) note that the underplating layer produced two distinct velocities from 7.0-7.5 km/s. The two most significant differences between the models are: 1) the representation of the underplating layer that extend approximately 600 km southward underneath the Wyoming Province before beginning to pinch out and 2) the presence of two north dipping reflectors.

Both velocity models, Figures 5 and 6, place the Moho depth beneath the Wyoming and Medicine Hat Block Provinces between 55 and 60 km. Both velocity models also indicate a high velocity ultramafic underplated layer, as well as a severely deformed lower crustal layer which perhaps marks the collision between the Medicine Hat Block and Hearne Archean provinces (Clowes et al. 2000; Gorman et al. 2000).

Magnetotellurics (MT) is a passive source geophysical technique that measures naturally occurring electrical and magnetic fields and can be used to model the electrical properties of the crust and mantle. Boerner et al. (1998) performed a MT experiment just northeast of the study area where the GFTZ intersects the Trans-Hudson Orogen (THO) in southern Alberta. The study showed that there was no preferred electrical strike direction except at mid-crustal depths where they became weakly 2-dimensional with conductive structures striking northeast (Boerner et al. 1998) parallel to the GFTZ. These strike direction results are consistent with the aeromagnetic anomaly fabric trends of the GFTZ (Boerner et al. 1998).

The Earthscope project, sponsored by the National Science Foundation, is a major seismic/MT experiment extending over the United States. Preliminary models from the MT data have shown a large resistive region between 150-250 km in depth that loosely coincides with the GFTZ (Meqbel et al. 2011). A similar resistive region has been imaged beneath the Slave Craton, with the possibility of being linked to economically important diamond sources (Jones et al. 2003).

1.40 Petrophysical Studies

Various studies have shown that some Archean cratons have experienced different geologic episodes of deformation and as a consequence, particular segments of a craton can have significantly different geochemical and isotopic characteristics (Mueller and Frost, 2006; Mueller, 2010). Isotopic differences are particularly useful in determining the sequence of events during which a craton has been created (Foster et al. 2006).

Based on isotopic data, early cratons have been divided into three different types: type I, type II, and type III. The Wyoming Province is an excellent example of a type III craton (Mueller, et al 1988). Type III cratons are highly differentiated, having undergone little to no early metamorphism and developing high $^{207}Pb/^{204}Pb$ ratios under these conditions (Mueller and Frost, 2006).

The Beartooth Mountains located on the northern edge of the Wyoming Province (Figure 1) exhibit enriched Pb isotopic compositions which indicate that the Wyoming Province has undergone a type of crust and mantle mixing that is found on Archean-aged cratons. The Beartooth Mountains range in composition from andesite to granite, however previous studies (Mueller and Frost, 2006) note that the andesite is of mantle origin, which supports the suggestion of a subduction environment. When considering the possibility of subduction, previous studies compared the isotopic signatures found within the Beartooth Mountains to modern subduction environments such as in Bali and Java. All three-share similar Pb isotopic characteristics and high field strength element depletion, which are linked to subduction related environments (Mueller et al, 1988).

1.50 Scope of Work

The lack of existing geophysical data present an opportunity to compile and analyze newly collected gravity, magnetic and MT data specifically focusing on the boundary between the Wyoming Province and the GFTZ. The GFTZ is a major tectonic feature formed between the collision of the Archean Wyoming Province and the Medicine Hat Block. The GFTZ may preserve the structural remnants of an ancient subduction environment extending under the Wyoming Province: interpreting the subsurface extent of this boundary relative to the adjacent and underlying Archean and Proterozoic structures is the focus of this study.

To provide gravity constraints on the subsurface structure of the boundary region, new gravity stations were collected at an interval that would allow for more detailed modeling and mapping across boundary between the Wyoming Province and the GFTZ. To aid in the interpretation of the gravity and magnetic data, horizontal derivative, band-pass filtered, and upward continuation maps were constructed. To obtain a more comprehensive representation of the subsurface across the boundary, two-dimensional (2-D) models were generated. The models and anomaly maps were interpreted in terms of the crustal and mantle structures within this region and are offered as one possible solution to the observed gravity and magnetic fields within the boundary.

Magnetotelluric data were also collected in conjunction with the new gravity transects to provide additional constraints. MT models provide additional information by measuring the electrical conductivity structure within the subsurface. To better understand the electrical structure, 2-D models were created.

Conducting such comprehensive geophysical analysis of the subsurface structure of this boundary has provided important constraints on the interaction of these structures relative to each other and their extent under the Phanerozoic cover. The findings of these models and the interpretation of the maps will be available for use in future studies within the region. This study investigates the major lithospheric blocks and their interactions in Northern Wyoming and Montana including the Wyoming Province, the THO, and the GFTZ.

2.0 GEOLOGIC HISTORY

2.10 Wyoming Province

The earliest origins of the Wyoming Province remain unknown due to the limited Archean outcrops and lack of deep geophysical studies within the Wyoming Province. In spite of these limitations there have been several interpretations, including; 1) the Wyoming Province is the southern continuance of the Archean Hearn Province in Canada, 2) it is an Archean microcontinent, or 3) it is a rifted portion of the Superior Craton that migrated westward while rotating 180° to its current orientation (Mueller and Wooden, 1988; Foster et al. 2006; Whitmeyer and Karlstrom, 2007).

The Wyoming Province is an Archean-aged craton located in the northwestern region of the United States (Figure 1). The core of the Wyoming Province is comprised of older (3.6-3.3 Ga) gneisses, that contain detrital zircons dating to 4.0 Ga (Chamberlain et al. 2003; Foster et al. 2006; Whitmeyer and Karlstrom, 2007) suggesting the existence of a craton at 4.0 Ga.

There have been numerous studies of the Wyoming Province and these studies have divided the craton into 3-5 distinctive terranes based on late Archean histories, see Figure 7; 1) the Montana Metasedimentary Province, 2) the Beartooth-Bighorn magmatic zone, and 3) the Southern Accreted Terranes. Other terranes include the Sierra Madre-Medicine Bow block (SM-MB) and the Hartville Black Hills, both of which are possibly allocthonous to the WP (Chamberlain et al. 2003; Mueller and Frost, 2006).

The Montana Metasedimentary Province is located in the northwestern section of the Wyoming Provinceand encompasses the oldest known Early to Middle Archean rocks of the Wyoming Province. Compositionally, the Montana Metasedimentary Province

contains quartzites, pelites, and carbonate rocks intermixed with older (3.50-3.30 Ga) quartzofeldspathic gneisses which are isotopically similar to the rest of the Wyoming Province (Chamberlain et al. 2003) (Figure 7). Shear zones along the southern edge of the terrane representing both the limit of magmatism from 2.9-2.75 Ga, and also marking the boundary of the subprovince (Chamberlain et al. 2003).

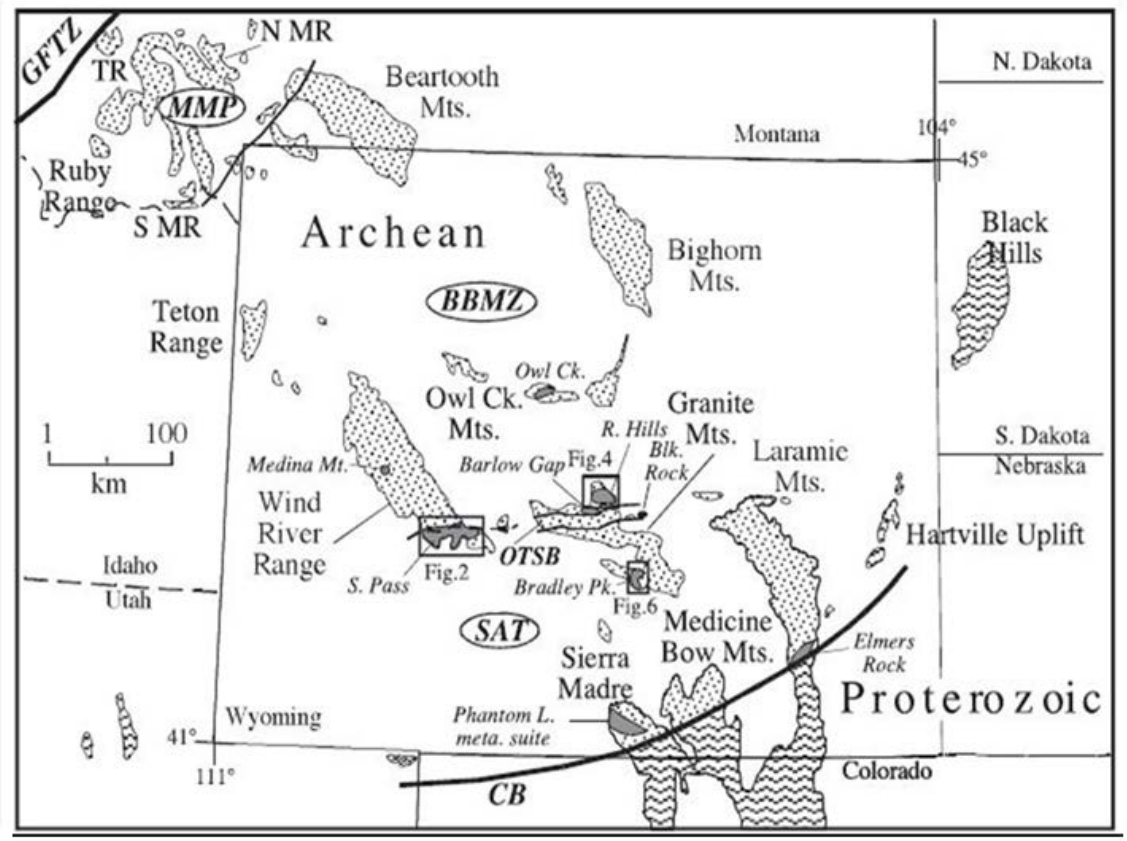

Figure 7. The location of the various terranes within the Wyoming Province. Archean rocks occur north of the Cheyenne Belt-DB and southeast of the Great Falls Tectonic-GFTZ. The Oregon Trail structural belt-OTSB separates the older rocks older rocks of the Beartooth-bighorn Magmatic zone-BBMZ and Montanta Metasedimentary province-MMP from the Southern Accreted Terranes-SAT. North Madison Range –NMR; South Madison Range – SMR; Tobacco Root Mountains-TR; Black Rock Mountain-BLK Rock; Rattlesnake hills-R Hills. Modified from Frost et al. (2003).

The Bighorn subprovince, which loosely coincides with the Beartooth-Bighorn magmatic zone, is located within the center of the WP (Figure 7). The Bighorn Mountains are one of the largest uplifts of the region with an Archean core (Mueller and Frost, 2006). Encompassing the northern region is the Bighorn batholith, dated to 2.8 Ga using U-Pb dating techniques, which is comprised of tonalite, granodiorite, granite, and quartz monzanites. Mineralogically and geochemically similar to the gneisses in the central Bighorn Mountains, the central and southern regions consist of gneissic terranes divided into three separate units; older quartzofeldspathic gneiss, a younger granitic intrusive complex, and a migmatite sequence in contact with the Bighorn batholith (Frost and Fanning, 2006).

Slightly younger magmatic and tectonic belts encompass the southern edge of the Wyoming Province with the SAT recording later Archean calc-alkalic magmatic and tectonic activity in three distinctive pulses between 2.71-2.50 Ga (Mueller and Frost, 2006). East to northeast directed subduction from 2.71-2.67 Ga resulted in a continental magmatic arc formation currently exposed in the Wind River Mountains along with a mafic dike swarm thought to represent a back-arc setting. Magmatism in this region continued from 2.65-2.50 Ga, in two distinct pulses. The first pulse occurring from 2.65-2.62 Ga in a more north directed subduction complex and the second pulse, from 2.55-2.50 Ga, was more extensive throughout the entire Wyoming Province but of less tectonic significance in terms of comparative volume of magmatism to the region (Frost et al. 2006). These later Archean sequences are composed of mafic and felsic metavolcanic rocks, metagraywacke, pelitic schist, minor quartzites, and iron depositions

which are believed to have originated as older detritus from possibly the BBMZ or MMP (Mueller and Frost, 2006).

The final two terranes within the Wyoming Province, the Sierra Madre-Medicine Bow Mountains and the Hartville-Black Hills uplifts, are suggested to be allocthonous based on basement gneiss ages found within each of the terranes (Chamberlain et al. 2003). It is believed that the Sierra Madre-Medicine Bow Mountains were accreted to the Wyoming Province by 2.62 Ga. Deformation during the Archean within the Phantom Lake suite may reflect the accretion to the craton in the form of southward dipping reflectors, evidenced in the CD-ROM experiment (Chamberlain et al. 2003). The Sierra Madre-Medicine Bow also experienced rifting between 2.1-2.0 Ga which caused thinning of the region along with numerous mafic dykes and sills throughout the region. The Hartville-Black Hills block is dominated by meta-sedimentary rocks. The Hartville-Black Hills uplifts underwent western directed deformation during the Proterozoic (2.62 Ga). The timing of these events are believed to be nearly coeval with the Medicine Bow orogeny within the Cheyenne Belt (Chamberlain et al. 2003; Frost et al. 2006).

2.20 Surrounding Archean and Proterozoic Terranes

The Wyoming Province is surrounded mainly by Late Archean- to Proterozoic-aged collisional belts and orogens including: 1) the THO, 2) Cheyenne belt, 3) Selway Terrane, 4) Belt Basin, and the 5) GFTZ. (Chamberlain et al. 2003; Foster et al. 2006; Mueller and Frost, 2006). The only non-Archean or Proterozoic terrane bordering the Wyoming Province is the basalts of the Snake River Plain (Figure 8) along its southwestern boundary.

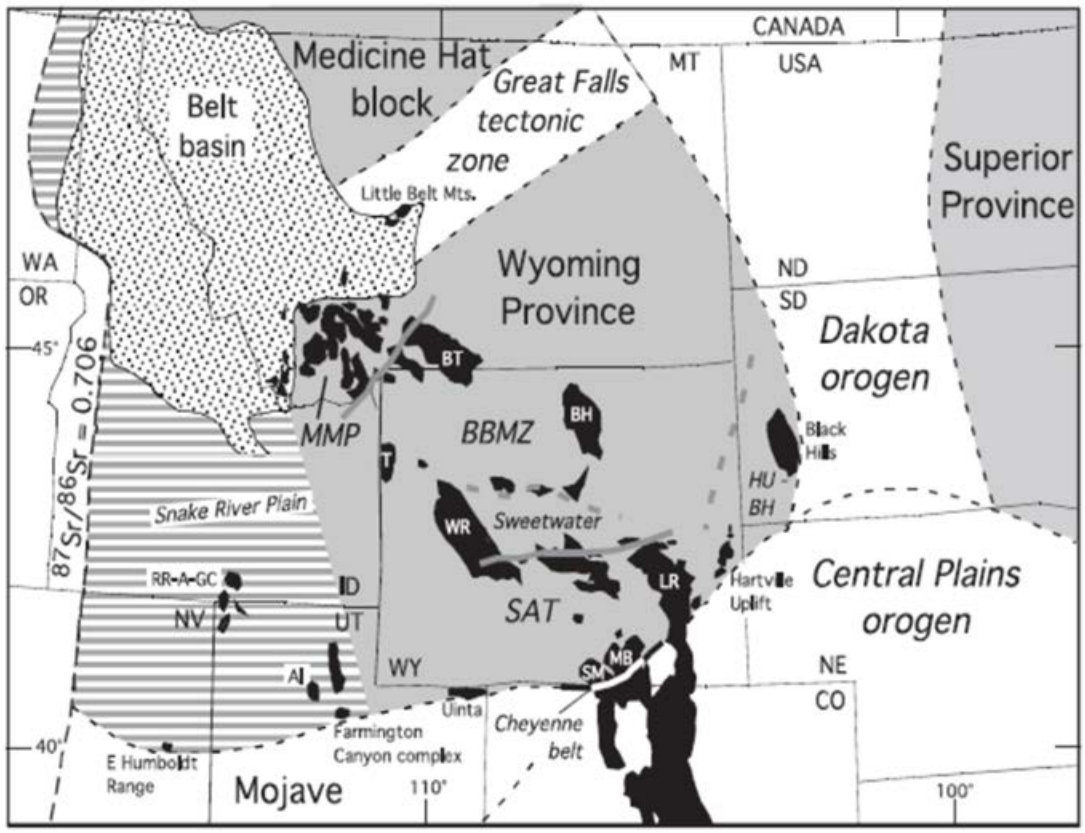

Figure 8. The Wyoming Province and its relationship to surrounding orogens and Precambrian provinces. Areas shown in black are Precambrian exposures. AI, Antelope Island; BH, Bighorn Mountains; BT, Beartooth Mountains; LR, Laramie Range; MB, Medicine Bow Mountains; RR-A-GC, Raft River – Albion – Grouse Creek Mountains; SM, Sierra Madre; T, Teton Range; WR, Wind River Mountains. Modified from Mueller and Frost, (2006).

The THO amalgamated to the Wyoming, Hearne, and Superior cratonic regions during the Proterozoic (1.82-1.78 Ga.) (Chamberlain et al. 2003; Foster et al. 2006; Whitmeyer and Karlstrom, 2007). The THO marks the closure of the Manikewan Ocean, an oceanic plate that once separated the Superior and Rae cratonic provinces (Whitmeyer and Karlstrom, 2007). The THO extends from South Dakota into northern Canada, in some regions widening to almost 500 km.

To the south lies a steeply dipping northeast-trending zone termed the Cheyenne Belt. The Cheyenne Belt is a Precambrian suture zone that helps form the southern

boundary between the Wyoming Province and the accreted Proterozoic terranes to the south. Occurring between 1.78-1.75 Ga. the Cheyenne Belt records the Proterozoic collision between the arc terranes with the Wyoming Province (Hoffman, 1988; Whitmeyer and Karlstrom, 2007).

The Farmington Canyon Complex is along the southwestern margin of the WP and constitutes the largest exposure of early Paleoproterozoic crust in the region. The FCC is comprised of quartzofeldspathic gneisses, migmatites, and metasedimentary rocks. While these are mostly Archean-aged rocks, zircons have been found that indicate deposition during the Early Paleoproterozoic (Foster et al. 2006).

Just to the north of the Farmington Canyon Complex lies the Selway Terrane. The Selway Terrane was proposed by Foster et al. (2006). The Selway Terrane covers the region underlain by Paleoproterozoic rocks west of the Laramide-aged uplifts of southwestern Montana. These Paleoproterozoic rocks crop out in north-south trending mountain ranges occurring along the eastern edge of the Sevier fold and thrust belt (Chamberlain et al. 2003).

The Snake River Plain is a northeast-trending volcanic region marking the path of the North American continent as it has migrated westward over the Yellowstone hotspot over the last 17 m.y. The Snake River Plain overprints portions of the Selway Terrane as well as a small portion of the western edge of the Archean Wyoming province in northern Wyoming (Leeman 1982) (Figure 8).

The GFTZ is a northeast trending zone of reactivated Archean rocks extending from southeastern Idaho, through Montana, and into southern Saskatchewan. The GFTZ is presumed to be the collisional point of the Wyoming Province and the Medicine Hat-

Hearne provinces. The western region of the GFTZ within the Little Belt Mountains, contain 1.86 Ga. calc-alkaline meta-igneous rocks exhibiting Nd isotope signatures suggestive of a convergent margin environment (Boerner et al. 1998; Foster et al. 2006).

The Belt Basin is geographically located in Idaho and western Montana and extends slightly into Canada. The Belt Basin was formed between 1500 to approximately 1320 Ma during the breakup of Rodinia and is associated with extensional faulting and magmatism that occurred during the accumulation history of the basin. It ranges in thickness from 2.5 km at the eastern end to approximately 12km thick in the Purcell Mountains (Sears, 2007; Winston and Sears, 2013).

The last major tectonic event occurring within the study region is the Laramide Orogeny. The Laramide Orogeny is a late Cretaceous to Paleocene (80-55Ma) orogenic event that is believed to be the result of flat slab-style subduction of the Kula-Farralon plate. The Laramide Orogeny involved Precambrian metamorphic basement rocks and affected areas as far as 750-1500 km inland from the nearest convergent margin.

3.0 GEOPHYSICAL DATA

3.10 Data Collection

G.P.S. Data Collection. In order to obtain the desired accuracy of the gravity readings of ± 0.1 mGal, the latitude and longitude of a gravity station must be known within 10 meters and the elevation within 1 meter. These types of accuracies can be accomplished using a differentially-corrected GPS (global positioning system) receiver capable of achieving ± 0.02-meter accuracy.

To obtain the above accuracies, GPS base stations must be used and permanent stations that occur throughout the survey region were used. The permanent GPS station at Lewistown, Montana maintained by the National Oceanographic and Atmospheric Agency (NOAA), as well as the six absolute base stations (Figure 9) were used to correct the data collected for this study. Base stations are needed to correct the station GPS data for atmospheric effects at the local station that will degrade the accuracy of the horizontal and vertical values. The processed GPS elevation data were then converted to geoidal elevations using the 2006 North American geoid.

Gravity Data Collection. The gravity data used for this study were obtained from two different sources. Figure 9 shows the location of the absolute base stations within the study area. The majority of the data were obtained from the National Geospatial and Imaging Agency (NGA), while the remaining data were collected by the author along the three profiles shown in Figure 10. The NGA data station spacing varies from 1 to 7 km, while the newly collected data have a station spacing varying from 1 to 2 km. The new data were acquired during June 2011 using a Lacoste and Romberg (L&R) Model G gravimeter with locations determined by a concurrent GPS survey. In order for the

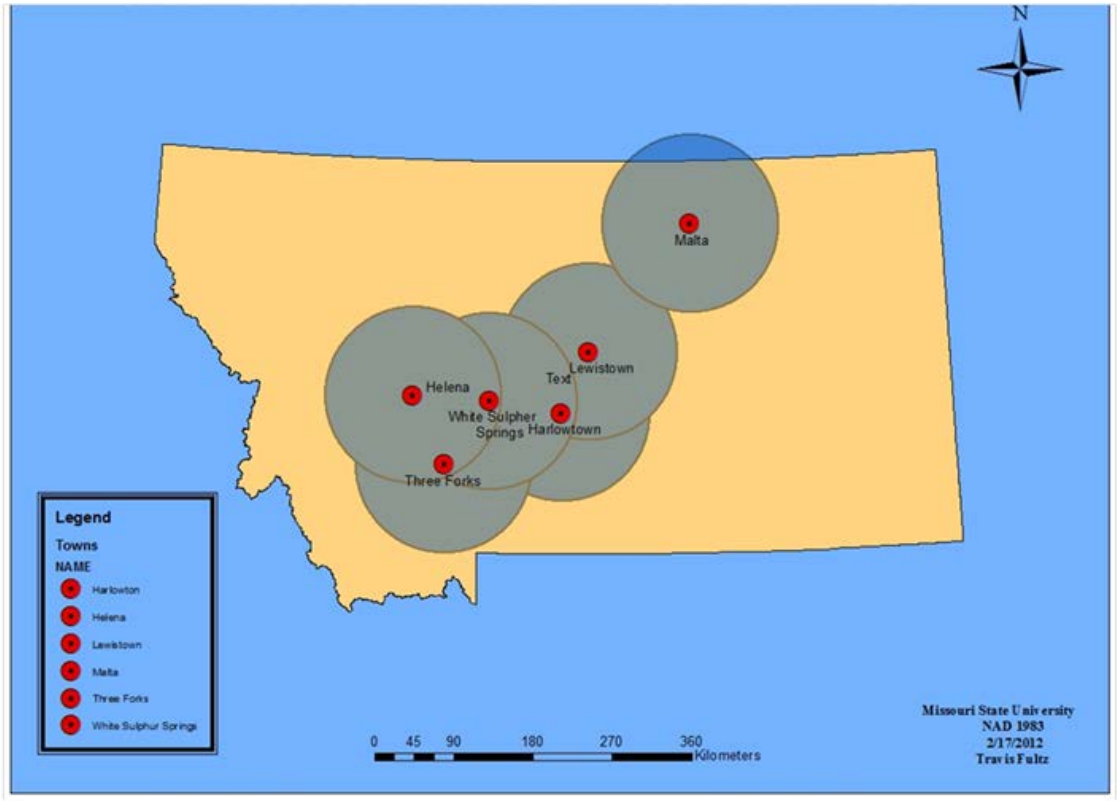

Figure 9. The six absolute gravity base station locations used to correct the data collected during the survey.

collected data to be included into the national databases the data must be corrected using the International Gravity Standardization Net 1971 (IGSN 71), along with a known absolute gravity station. Additionally, a local base station is also needed. The local base station is used to correct for gravimeter drift throughout the day as data are collected. The local base stations were collected twice each day, at the beginning and ending of each day. At least once during the survey the local base station must be tied into the absolute gravity station (Figure 10).

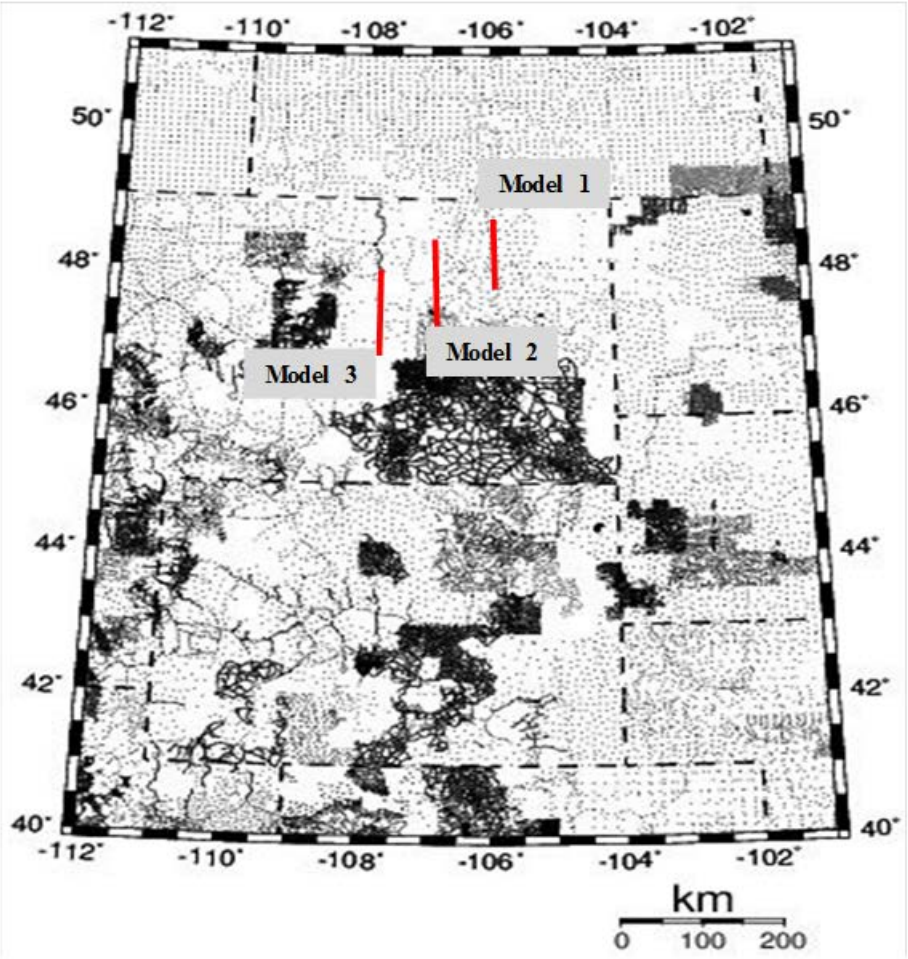

Figure 10. The distribution of all gravity points within the study area, both from existing databases and the newly acquired profiles. Red lines show the location of the newly collected data.

Magnetic Data Collection. The aeromagnetic data were obtained from the USGS (Bankey et al. 2002). The data were merged from numerous airborne surveys into a 1 km grid with flight spacing ranging from 4 to 8 km. In this survey, the regional effects of the earth's magnetic dipole were removed such that the residual magnetic anomalies represent variations in the subsurface mineralogy and petrography. The data were processed by the USGS source to remove the effects of the earth's main dipolar field using the International Geomagnetic Reference Field (IGRF).

Magnetotelluric Data. The MT method uses time-varying electromagnetic fields. These fields are produced by two different sources: 1) the interaction between the sun's solar winds with the earth's magnetosphere and ionosphere, and 2) variations produced by storms on the surface of the earth, in the form of lightning storms. These field variations, depending on the frequencies recorded, are capable of penetrating to upper mantle depths.

For this study, MT data were obtained through the IRIS Data Management Center (DMC) and were recorded by the NSF Earthscope project. IRIS DMC is the access point for data received from the US Array, Earthscope's transportable array MT component.

Data collection was facilitated through the use of a Narod Intelligent Magnetotelluric System (NIMS), which is a digital recording long period MT receiver with a data logger. The nominal bandwidth of the NIMS is from 2 to 36,000 seconds, and can be configured to record at either 1 Hz or 8 Hz. The remaining components of the Earthscope transportable array are a three-component magnetometer and two horizontal electric dipole receivers. MT data were collected over a period of 21 days at each station with stations spaced in a 70x70 km grid (Figure 11).

3.20 Data Processing

Gravity Data Processing. Before the raw gravity data can be used to interpret Earth structures, all known gravitational effects must be removed. The L&R gravimeter uses an internal metal spring to measure the gravitational field at each station. Throughout the day this spring will undergo elastic creep related to thermal expansion and contraction, along with mechanical tensioning and releasing, therefore these variations must be accounted for during processing. By establishing a local base station,

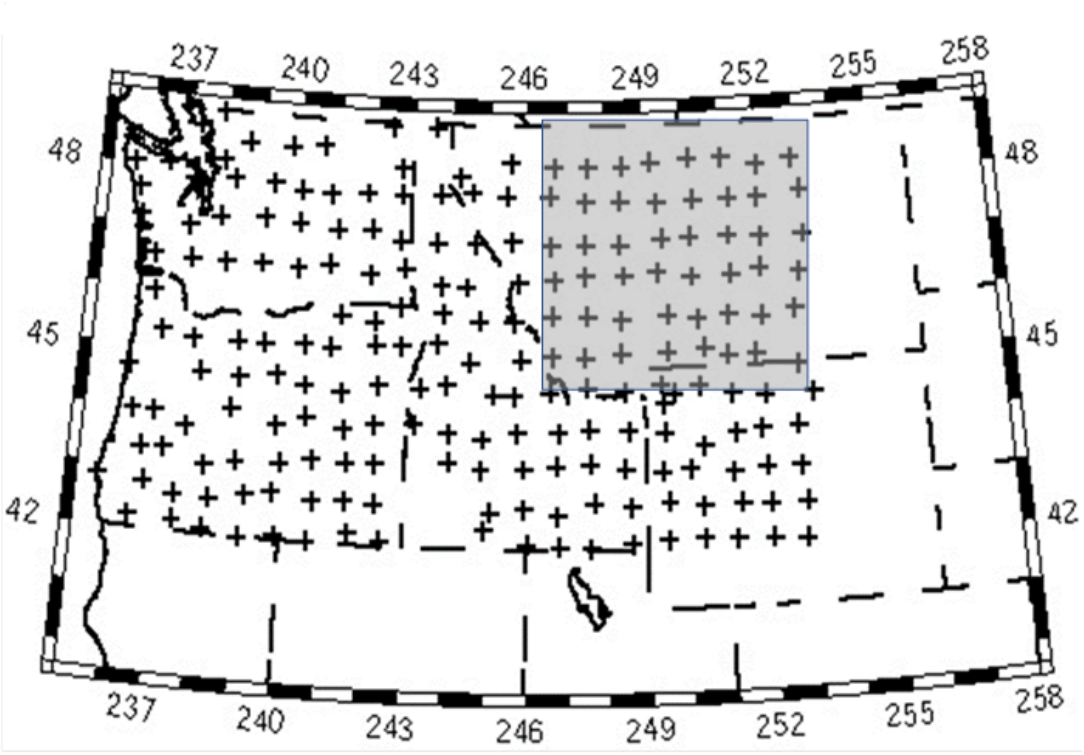

Figure 11. The location (+) of the Earthscope transportable MT stations through 2009. The shaded area shows station locations used for this study.

the meter drift can be calculated and corrected. By calculating the difference in the beginning and ending values, the remaining survey points are adjusted upward or downward to obtain the corrected meter reading. Once collected and translated into usable values (corrected for daily instrumental drift) and referenced to the 1971 IGSN Net, the data are ready to be processed to produce Bouguer gravity anomaly values.

Because the Earth is an oblate spheroid, with the radius being greater at the equator, gravitational forces are directly proportional to the distance from the center of the earth. To correct for the variations in gravity due to latitudinal variation the 1967 International gravity formula was applied using latitude data gathered from the GPS

survey. The latitude data were processed using the World Geodetic System 1984 geographic coordinate system.

Just as there are variations in gravity due to changes in latitude, there exist variations due to changes in elevation. The changes result from increasing distance from the geoid. To account for these changes, the free-air-correction (FAC) was applied to the observed gravity values. The FAC is the difference between gravity recorded at sea level and that measured at a certain distance above the reference elevation with no rock in between (Reynolds, 1997). For most surveys, the reference elevation is mean sea level. In order to correctly apply the FAC, the exact station elevation must be known. For this survey the elevation was obtained from the GPS survey as illustrated in Figure 12.

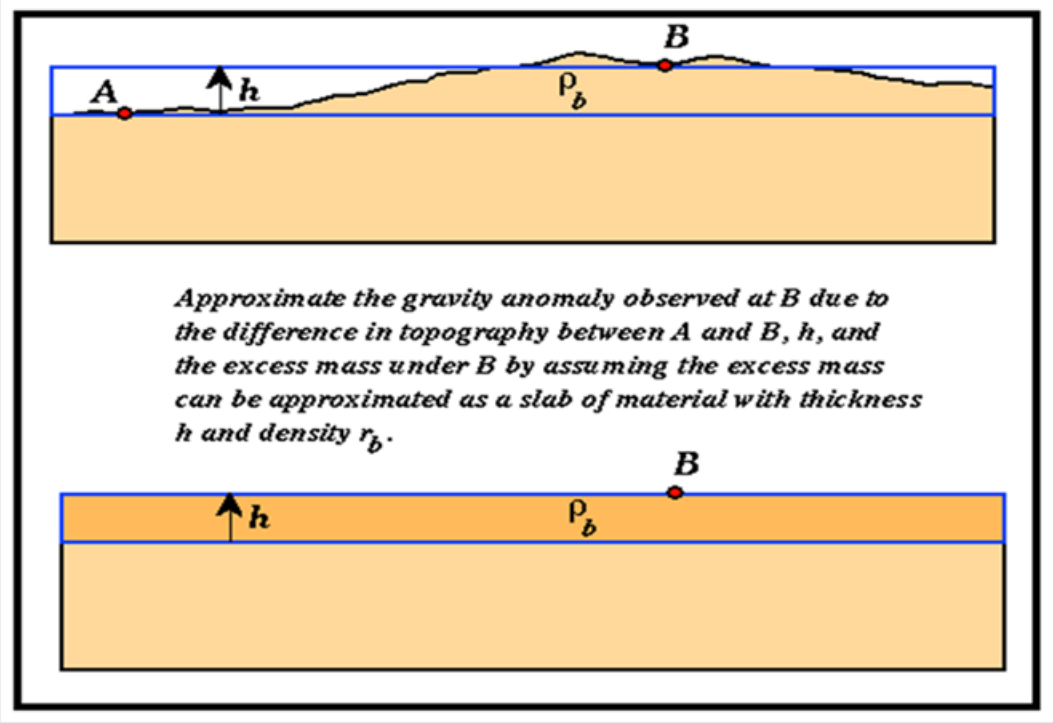

Figure 12. The concept of the Bouguer gravity correction. Reynolds (1977).

The Bouguer correction is implemented to compensate for the increased gravitational forces exerted by a rock slab of "h" thickness, of density ρ (kg/m^3) (Figure 12). Since the Bouguer correction overestimates the density of $g_{(obs)}$ it must be subtracted out for stations above sea level. To calculate the Bouguer correction value the following equation is used (Reynolds, 1997):

Bouguer Correction (δg_B) =2ΠGρh=βρh (g.u.), where:

B=2ΠG=0.4192 g.u.

G=6.67 x 10^{-8} m^3 Mg^{-1} s^{-2} and density (ρ) measured in Mg m^{-3} and height (h) is measured in meters.

In surveys where there are minor topography variations, the FAC and Bouguer corrections are sufficient to compensate for variations in gravity. However, there are few regions without variations in topography. The Bouguer correction assumes an infinite slab of uniform density; it negates any variations from nearby hills and valleys, necessitating a terrain correction. The effects of topography are shown in Figure 13.

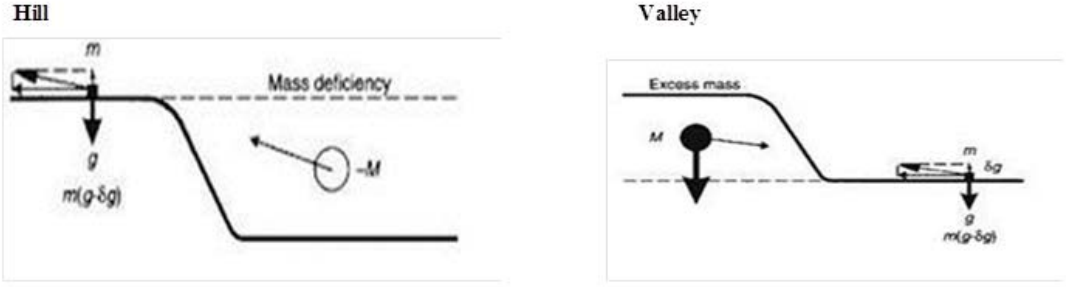

Figure 13. Diagram illustrating the effects of a hill and valley on gravity measurements and the need corrections. Modified form Reynolds (1977).

To correct for these variations in topography, the physical deviations of each station site are recorded on Hammer Terrain Correction charts (Hammer charts) (Figure 14). The Hammer chart is superimposed over a topographic map and the average elevation is estimated within each zone. When surveys are performed above sea level the Hammer chart values are added to the final Bouguer anomaly value (Hammer, 1938) (Figure 14). For this survey the terrain corrections within the zones of B and C were estimated in the field, the terrain corrections for the outer zones were estimated using 10 and 30-meter digital elevation models (DEM) and a computer algorithm (Nagy, 1966). The end result is the complete Bouguer gravity anomaly.

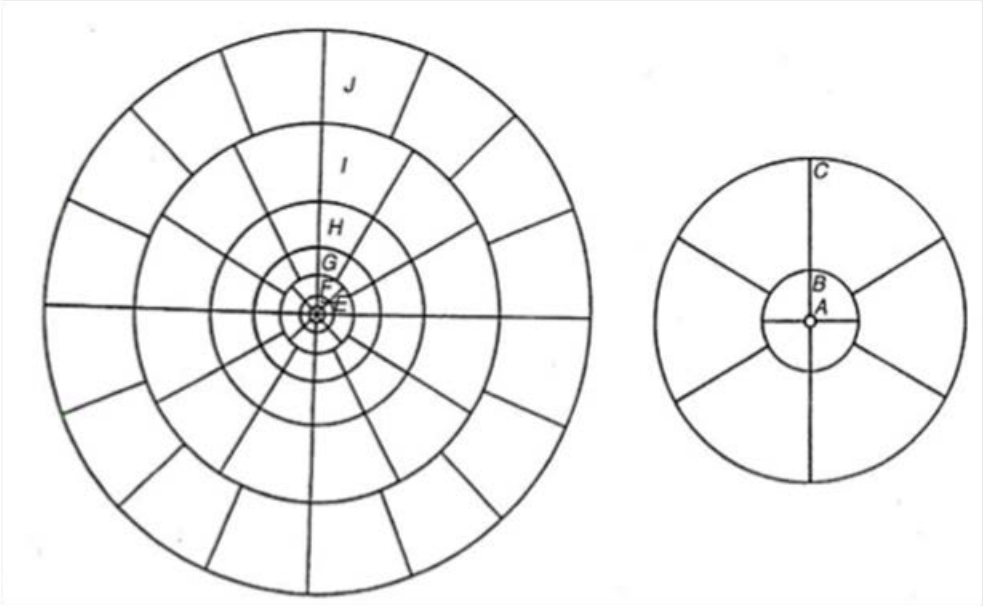

Figure 14. Typical Hammer Chart, with only the inner segments, B and C, were recorded in the field. Modified from Reynolds, (1997),

Magnetotelluric Data Processing. The objective of MT data processing is to extract smooth, repeatable functions representing the earth's response from raw noise-like signals and to use the resulting data to create interpretations of earth's conductivity structure. All initial noise processing followed a technique developed by Egbert (1997).

Sounding curves were plotted as log-log plots that relate apparent resistivity and phase variations as a function of period. Longer periods correspond to greater depth penetration resulting from longer wavelengths; however, the increased depth penetration results in increasingly inaccurate data. The majority of errors typically occurred in the longer wavelength soundings which extended out to periods of 10,000 to 30,000 seconds (Figure 15). Data points with large errors were removed from subsequent analyses.

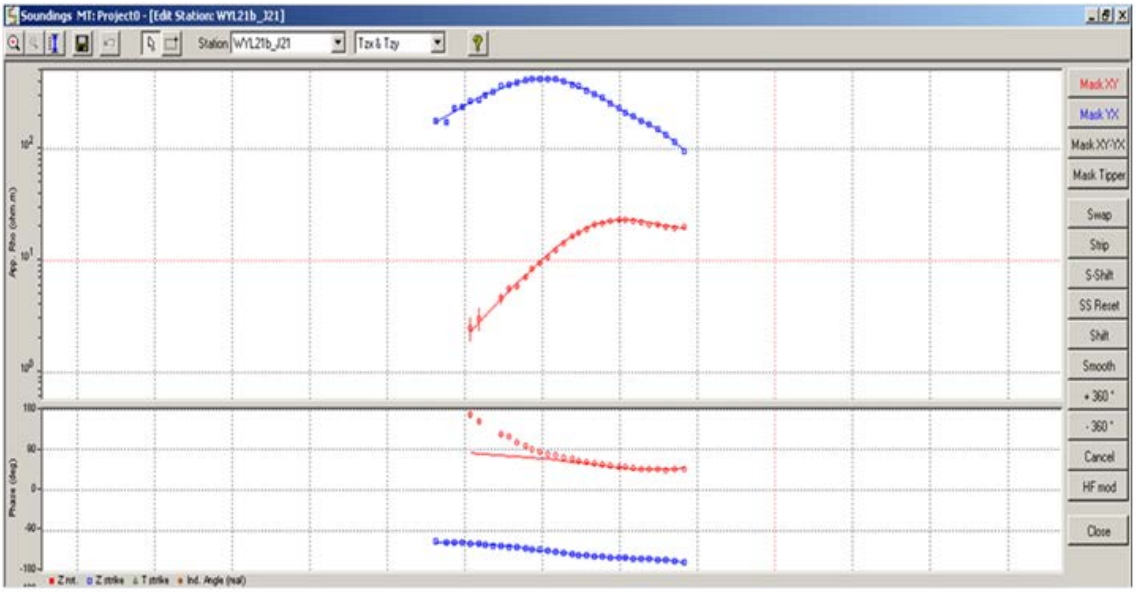

Figure 15. Figure shows an example of the sounding curves produced during processing. The upper plot shows apparent resistivies (dots) in ohms-meter,

4.0 DATA ANALYSIS

The recently collected gravity data from within the GFTZ and surrounding area were combined with existing data, gridded, and contoured to produce a complete Bouguer gravity anomaly map (Figure 16). To aid with regional interpretation, magnetic intensity data were gridded and contoured to produce a magnetic map (Figure 17). These maps, along with the regional MT profiles, illustrate the geophysical characteristics of the Wyoming Province and GFTZ regions and the surrounding terranes.

To assist in interpreting the gravity and magnetic data numerous methods can be used to enhance anomaly features. These include isostatic gravity residual anomalies, upward/downward continuation, wavelength filtering, and horizontal derivatives. Although different methods were incorporated for this study, only those maps that highlighted particular features are included here. The following pages discuss the interpretations of the complete Bouguer gravity anomaly and residual gravity and magnetic anomaly maps.

4.10 Regional Gravity

As illustrated on the Bouguer gravity anomaly map in Figure 16, the study area has strong gravity gradient variations. Perhaps the most prominent attribute of the map is the large scale southwest to northeast broad semi-linear gentle trend that crosses the entire region; trending from gravity minimum (low mGal) values in the southwest region, anomaly A-which corresponds to the WP, and continuing as a broad linear pattern to the northeast region of the map where the gravity maximum values occur, anomaly B-which corresponds to the THO. These broad low gradient trends are associated with long wavelength anomalies, which may be associated with deeper seated crustal features

(Reynolds, 1997). Anomaly C corresponds to the GFTZ and is believed to trend as it extends from southern Saskatchewan, through Montana, and southeast into Idaho.

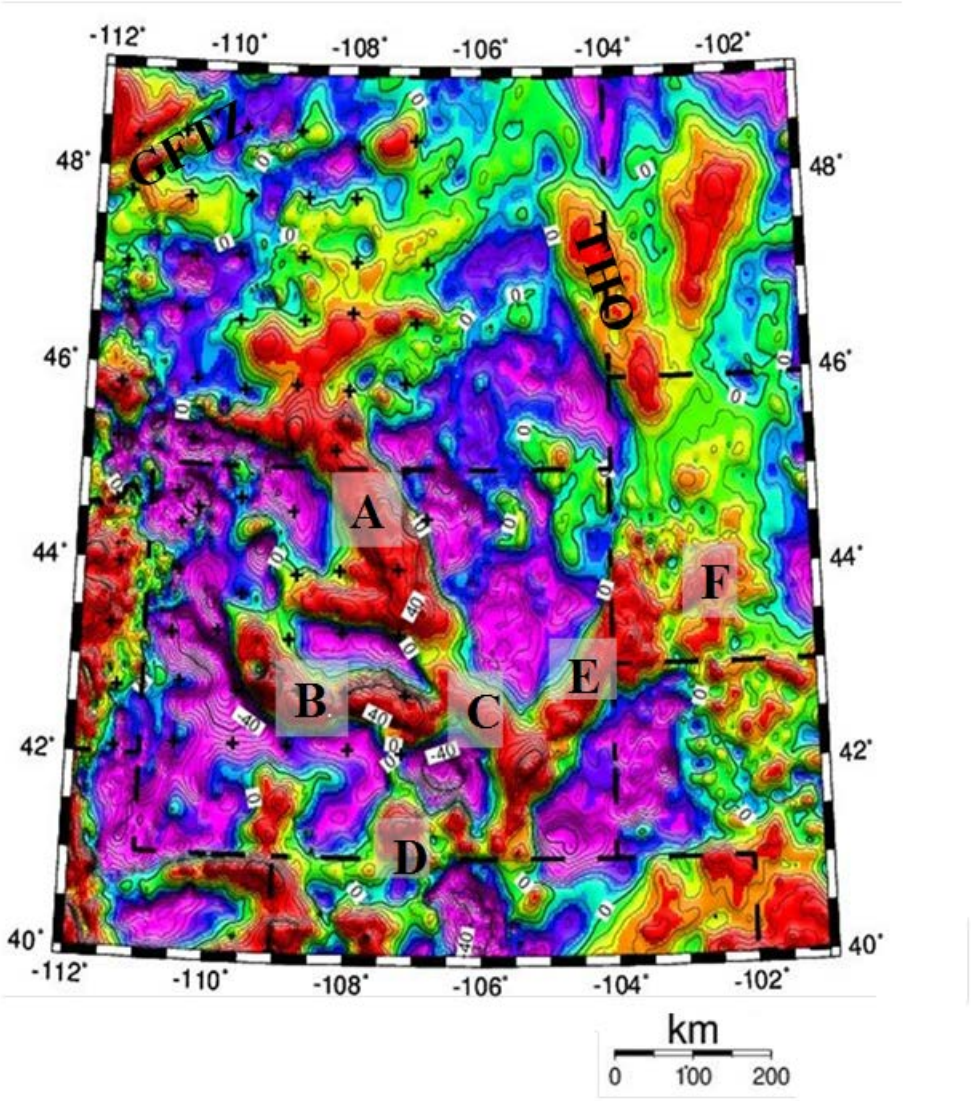

Figure 16. Bouguer gravity anomaly map. The major features are: A) the Wyoming Province, B) the Trans-Hudson Orogen, and C) the Great Falls Tectonic Zone. Contour interval is 10 mGal.

4.20 Magnetics

The regional magnetic intensity map does not appear to share the same broad trending anomalies as seen on Bouguer gravity anomaly map. Although not as apparent, distinctive magnetic anomalies are distinguishable. In Figure 17, two distinctive linear anomalies can be identified, along with a centrally located circular feature. Occupying the central region of the map is anomaly A, a large circular feature. This circular anomaly is interpreted as the outline of the WP. Anomaly B is a north-south linear trending anomaly corresponding to the THO. The boundary for the THO extends from Saskatchewan southwest along the western border of South and North Dakota, adjacent to the Black Hills.

Anomaly C is a southwest-northeast linear trending anomaly representing the GFTZ. Linearity of the anomaly patterns can often be an indicator of the strike direction of structures, and commonly can be associated with MT-generated electrical strike directions. Interestingly one can also see where the THO trend truncates that of the GFTZ right around 106° longitude and 50° latitude, indicating that the THO is younger than the GFTZ.

4.30 Residual Gravity and Magnetics

Residual Gravity. A useful technique in map analysis and interpretation is wavelength filtering. The most common method is band-pass filtering where user defined (either short or long) wavelengths can be either enhanced or eliminated. Low pass filters are designed to remove shorter wavelength anomalies and this type of filtering is useful

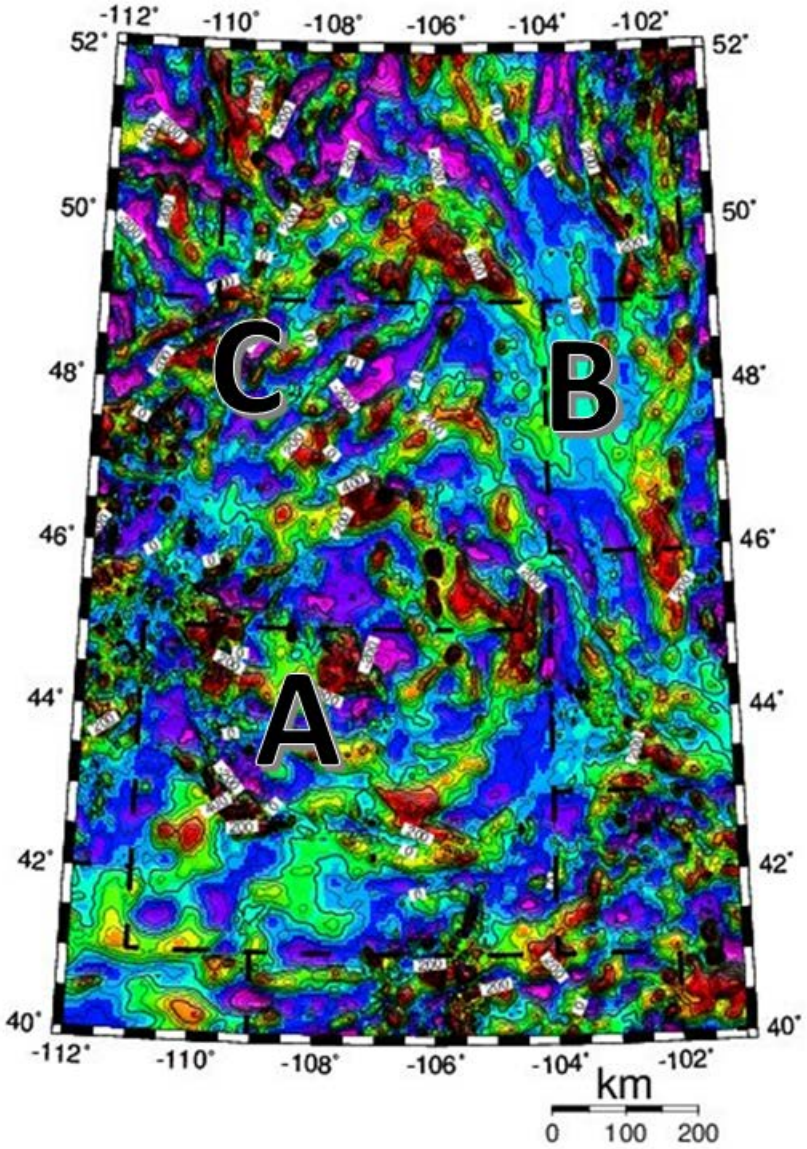

Figure 17. Total field magnetic intensity map of the study region. The major features outline are: A) the Wyoming Province, B) the Trans-Hudson Orogen, and C) the Great Falls Tectonic Zone. Contour interval is 100 gammas.

for smoothing out noisy data and to enhance deeper density structures. High pass filtering removes long wavelength anomalies generally associated with deeper seated features (Reynolds, 1997) and enhances shallow crustal generated anomalies.

Figure 18 presents a residual gravity anomaly map produced through band-pass filtering. This map was produced by passing wavelengths between 10 and 100 km in an attempt to remove the deeper-seated features related to Archean-aged structures. The remaining anomalies are related to Laramide-age deformation (anomalies A to F). The most prominent feature is the positive anomaly related to the Beartooth Mountain range, a 2.80-3.00 Ga composition of trondhjemite-tonalite-granodiorite rocks (anomaly A). Other notable anomalies are associated with the Laramide uplifts including the Wind River Mountains (anomaly B), the Laramide Range (anomaly C), the Sierra Madre (anomaly D), the Hartville Uplift (anomaly E) and the Black Hills uplift (anomaly F). Although high-pass filtering removes long wavelength anomalies, this technique was unable to remove Laramide-aged anomalies completely, possibly as a result of the involvement of underlying basement rocks during deformation, or by the large-scale nature of the features themselves with wavelengths long enough to overshadow Archean age gravity effects.

Residual Magnetics. Figure 19 presents the results from applying the wavelength filtering method to the magnetic maps, thereby producing a residual magnetic anomaly map. On this map, wavelengths from 25-50 km were passed, however this filter did not produce dramatically different results from the regional magnetic anomaly map (Figure 17). On Figure 19, the four labeled anomalies (A-D) are enhanced slightly. Both of the linear anomalies, the THO (B) and GFTZ (C), are easily identifiable, most notably in the area where the THO truncates the GFTZ.

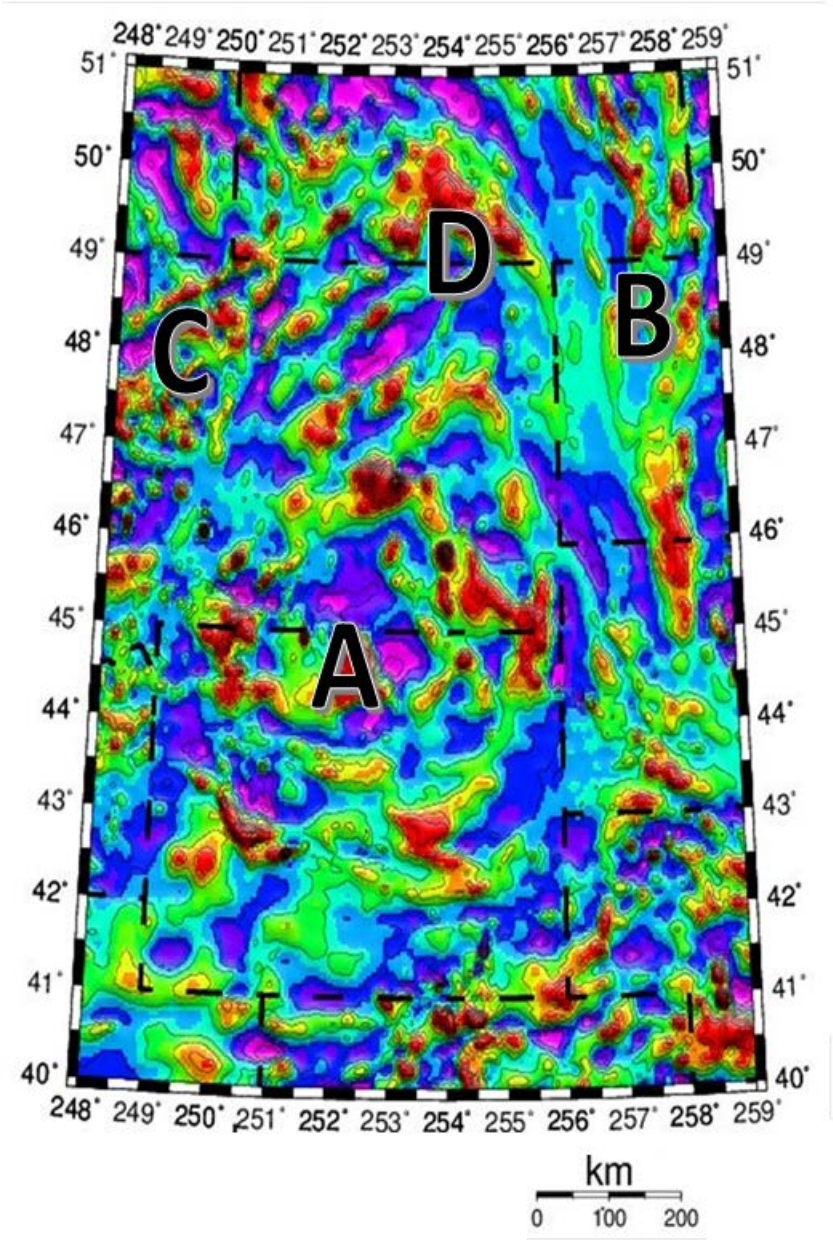

Figure 18. Residual gravity anomaly map created by using bandpass filtering were wavelengths between 10 and 100 km were passed. Contour intervals are 10 mGal. Major features identified are the A, Beartooth Mountains; B, Wind River Mountains; C, Laramide Range: D, Sierra Madre: E. Hartville Uplift; F, Black Hills; the THO, and GFTZ features. Black crosses depict MT station locations.

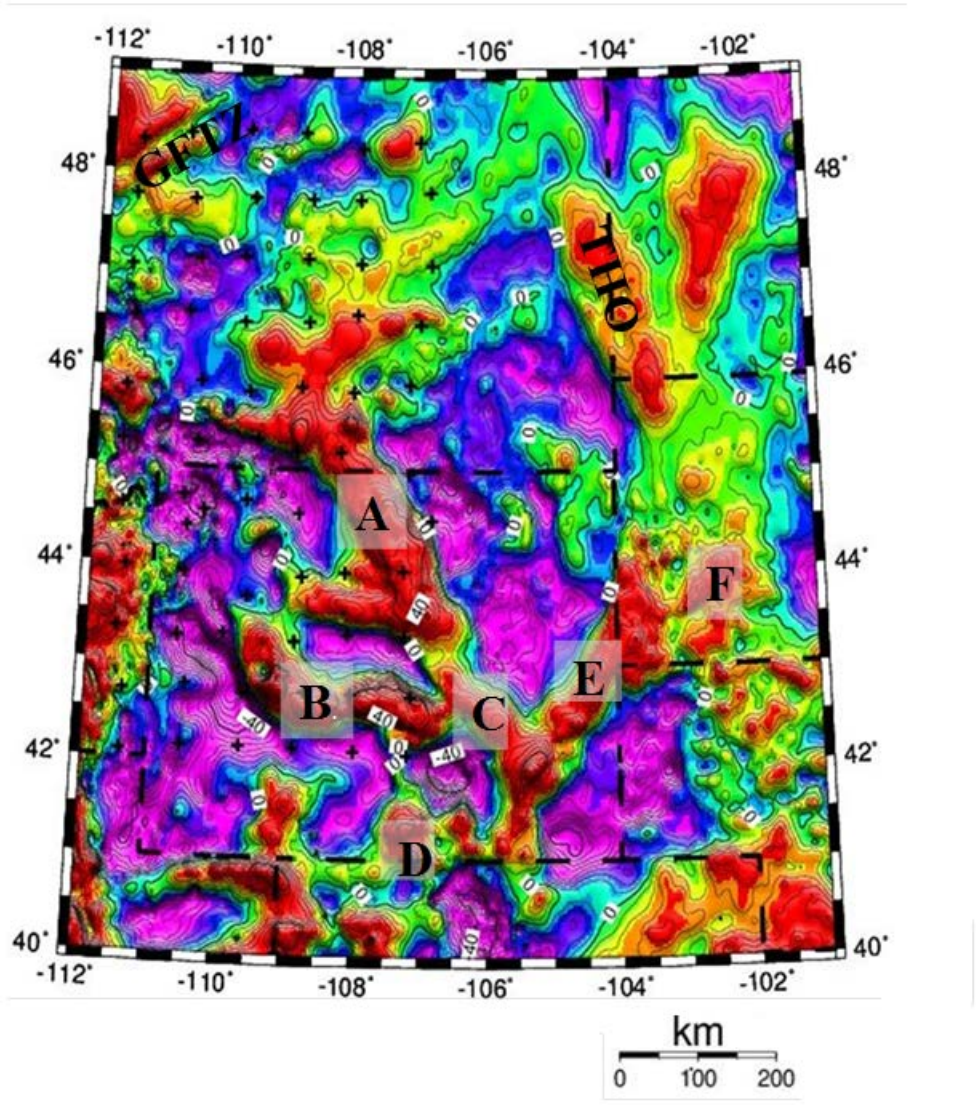

Figure 19. Residual magnetic anomaly map created using bandpass filtering. Wavelengths of 25 and 50 km were removed. Contour interval is 100 gammas. The major features outlined are: A) the Wyoming Province, B) the Trans-Hudson Orogen, C) the Great Falls tectonic Zone, and D) a magnetic high.

Figure 20 presents a second, band-pass filtered map where wavelengths between 150 and 250 km were passed. This map emphasizes deeper or broader magnetic sources. The GFTZ remains identifiable through the strong linearity that is still visible suggesting

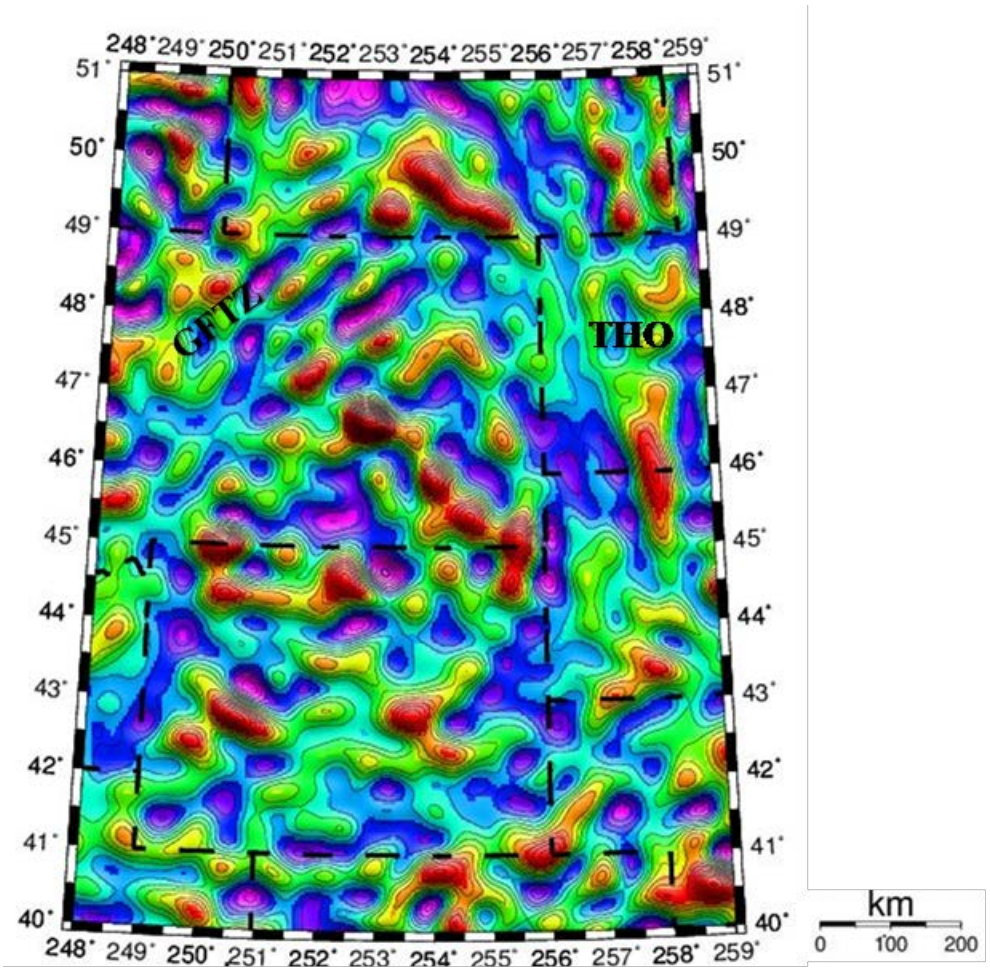

Figure 20. Residual magnetic anomaly map created using bandpass filtering. Wavelengths 150 and 250 km were passed. Contour interval is gammas.

it is a deep-seated feature. The GFTZ and the THO remain somewhat identifiable as well as anomaly D from the previous band-pass map (Figure 19).

4.40 Upward Continuation of Gravity

Upward continuation transforms the potential field that is measured at one surface to the field that is measured on another (Reynolds, 1997). Upward continuation attempts to attenuate the shorter wavelength features, the shorter the wavelength, the greater the

attenuation. As mentioned earlier, one of the problems with performing gravity and magnetic transformation codes on gravity data in this region results from the high amplitude anomalies caused by Laramide-aged deformation. Because the Laramide deformation resulted from flat slab subduction, the basement rocks within the WP were involved to a greater degree than normal subduction would have been. Trying to filter out Laramide deformation related anomalies resulted in filtering out anomalies caused by some Archean features as well. Figure 21 shows an upward continuation gravity anomaly map, where the gravity anomalies were continued upward 5km. However, due to the deep-seated nature of the Laramide deformation the upward continuation filtering could not separate out Archean features from the Laramide deformation.

4.50 Horizontal Derivative Gravity Maps

The horizontal derivative gravity maps are produced to assist in delineating edge effects or subsurface boundary features of varying densities (Fedi and Florio, 2001). The edge delineation procedure was applied to the complete Bouguer gravity anomaly gridded data. The result of the enhanced horizontal gradient (EHG) shows gradient as mGal/km, and high density contrasts within the subsurface are displayed as higher values. In Figure 22, the horizontal derivative map highlights remnants of; the THO, the Beartooth Mountains, the Wind River Mountains, the Hartville Uplift-Black Hills, the Sierra Madre Mountains.

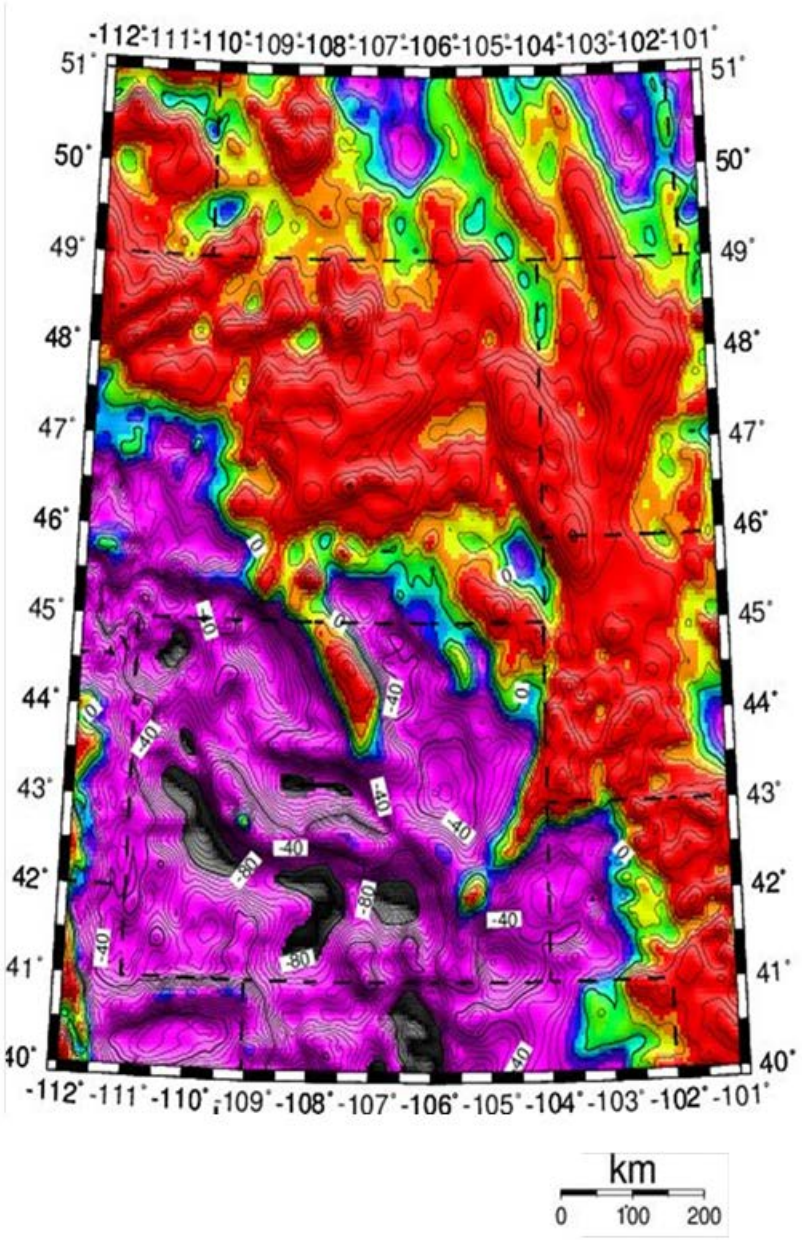

Figure 21. Residual gravity anomaly map created by upward continuing the Bourger gravity anomaly data to 5 km. Contour interval is 10 mGal.

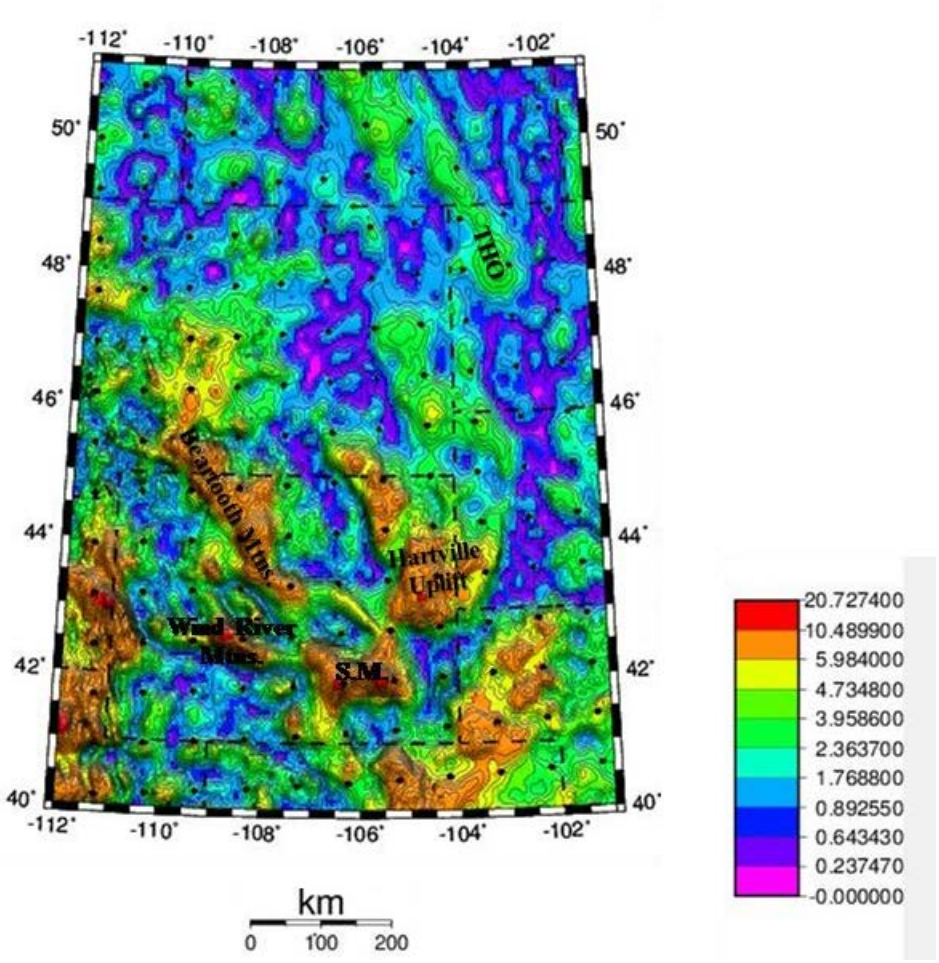

Figure 22. Horizontal derivative gravity map created by filtering the horizontal derivative. Contour interval is 1 mGal/km. Features highlighted are Laramide uplifted mountains including the Beartooth Mountains, the Wind River Mountains, the S.M., the Hartville Uplift as well as the THO. Black dots represent MT station locations.

5.0 MODELING AND DISCUSSION

In order to develop a more complete understanding of the region three two-dimensional (2-D) gravity models and three 2-D MT models were created. The gravity profiles were selected based on the MT data station locations shown in Figure 10. Seismic velocities and models obtained from both SAREX and Deep Probe data were utilized for constraints (Clowes et al. 2000; Gorman et al. 2002). The seismic p-wave velocities from the above models were converted from known rock densities. These densities along with average values for surface rock units (Reynolds, 1997) were used as starting values and were varied within 10% during the modeling process. Geological models based on mapping, geochemistry and isotopic studies were also used in constraining the models (Mueller and Wooden, 1988; Mickus, 2007; Mueller et al. 2011). The final models were developed through a trial and error process until calculated gravity anomalies approximately fitted the observed gravity values.

5.10 Gravity Modeling

Model 1 Profile 106° (Figure 23) is approximately 470 km long and extends roughly from north of Glasgow, Montana south along State road 24. This line includes 60 gravity stations where the Bouguer gravity anomaly values range from -88 mGal to -71 mGal. The crustal thickness ranges from 48 to 52 km, thickening to the southwest based on the Deep Probe models. The upper crust thickens toward the south while the lower crust thins. The thicker upper crust is found near the northern boundary of the WP and may have been caused during a southward subduction. The underplating layer is relatively thin compared to the 20-km thick layer found by the Deep Probe project (Gorman et. al. 2000).

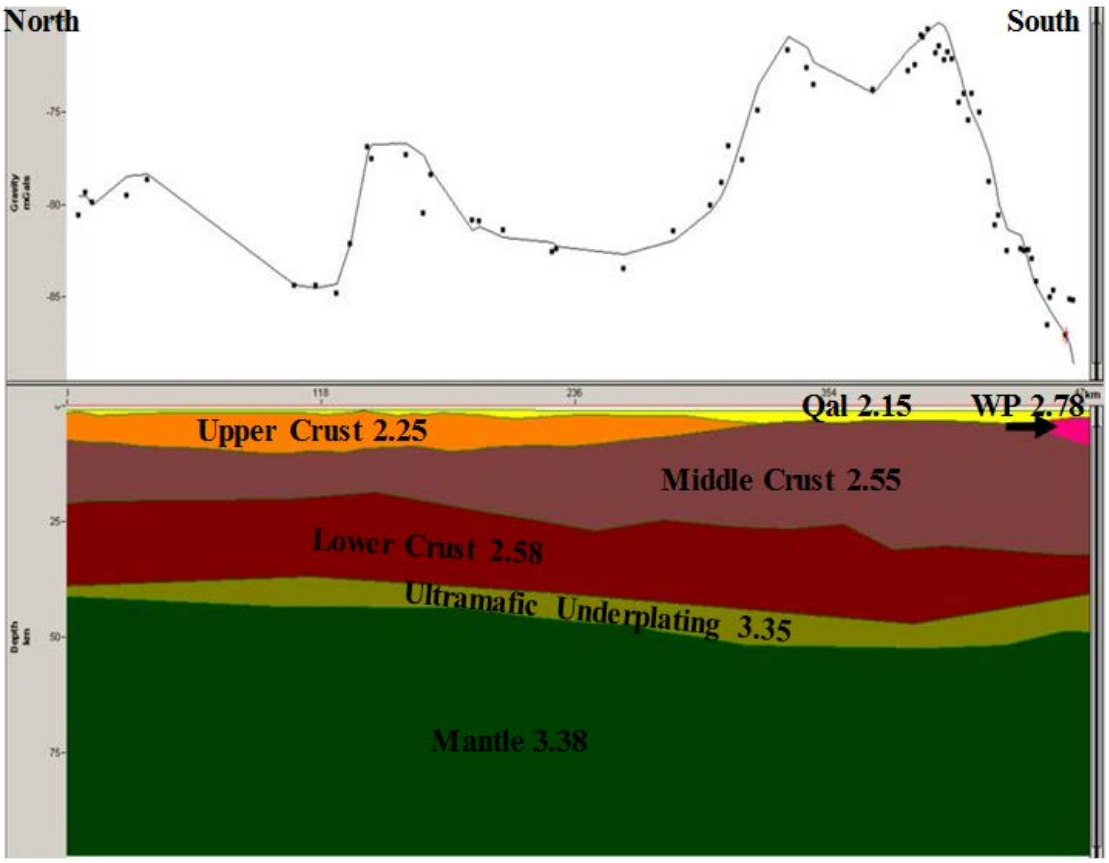

Figure 23. Model 1 showing gravity model along the 106° longitude line. The black dots are observed gravity values. The solid line represents the calculated gravity value. WP. Wyoming Province.

Model 2 (Figure 24) is approximately 530 km long and extends from north of Malta, Montana southward, along highway 191. This line includes 51 gravity stations where the Bouguer gravity anomaly values range from -132 mGal to -72 mGal. The crustal thickness ranges from 48 to 61 km, thickening to the southwest. In contrast to model 1 (Figure 23), the upper crustal layer thickness does not vary and the underplated material is thicker which agrees well with the thickness found by the Deep Probe project.

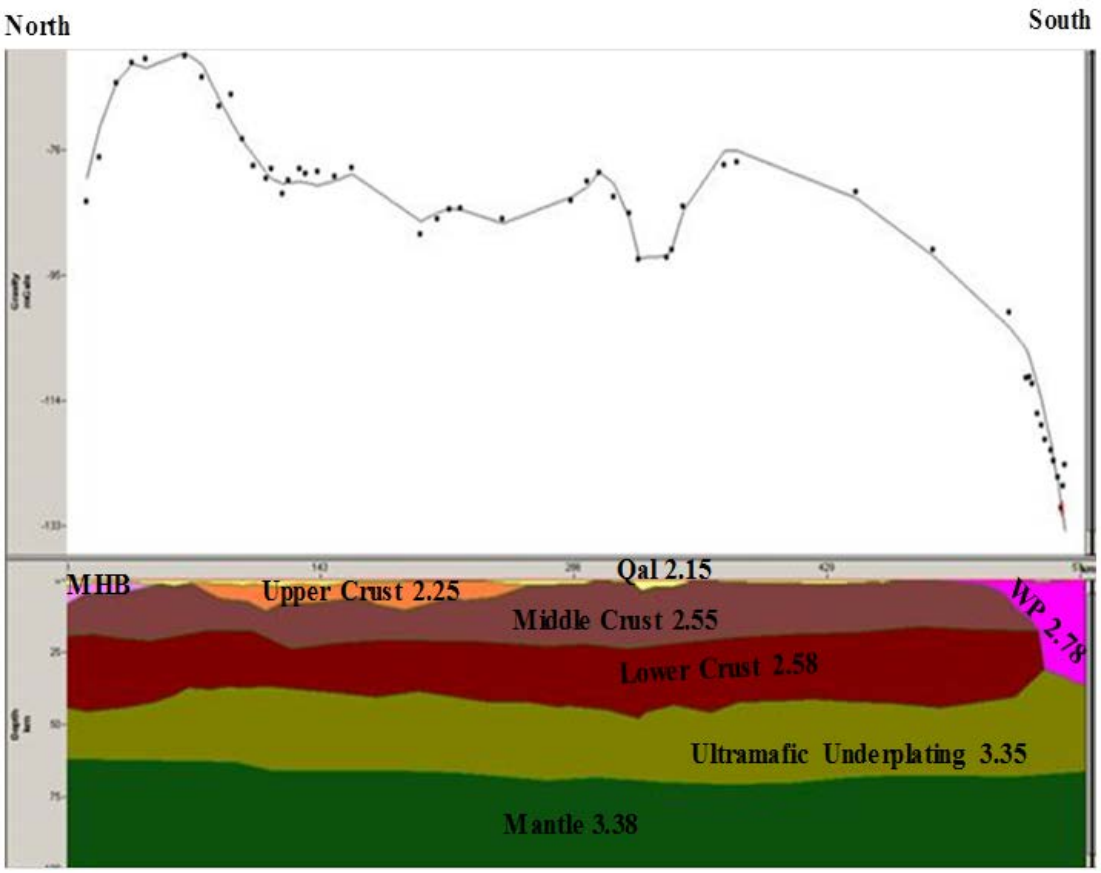

Figure 24. Model along 107° longitude line. Solid line depicts calculated gravity value. Black dots represent actual gravity measurement. The solid line represents the calculated gravity value. MHB, Medicine Hat Block-2.78.

Model 3 is approximately 514 km and extends from south of Havre, Montana southwards along highway 87. This profile consists of 93 gravity stations where the Bouguer gravity anomaly values range from -113 mGals to -63 mGals. The crustal thickness ranges from 35 to 52 km in this region. Model 3 has similar crustal geometries and thickness as model 2 (Figure 25). The underplated material is thicker than found on model 2 suggesting that the Archean crust has greater modification in this region of the Wyoming Province.

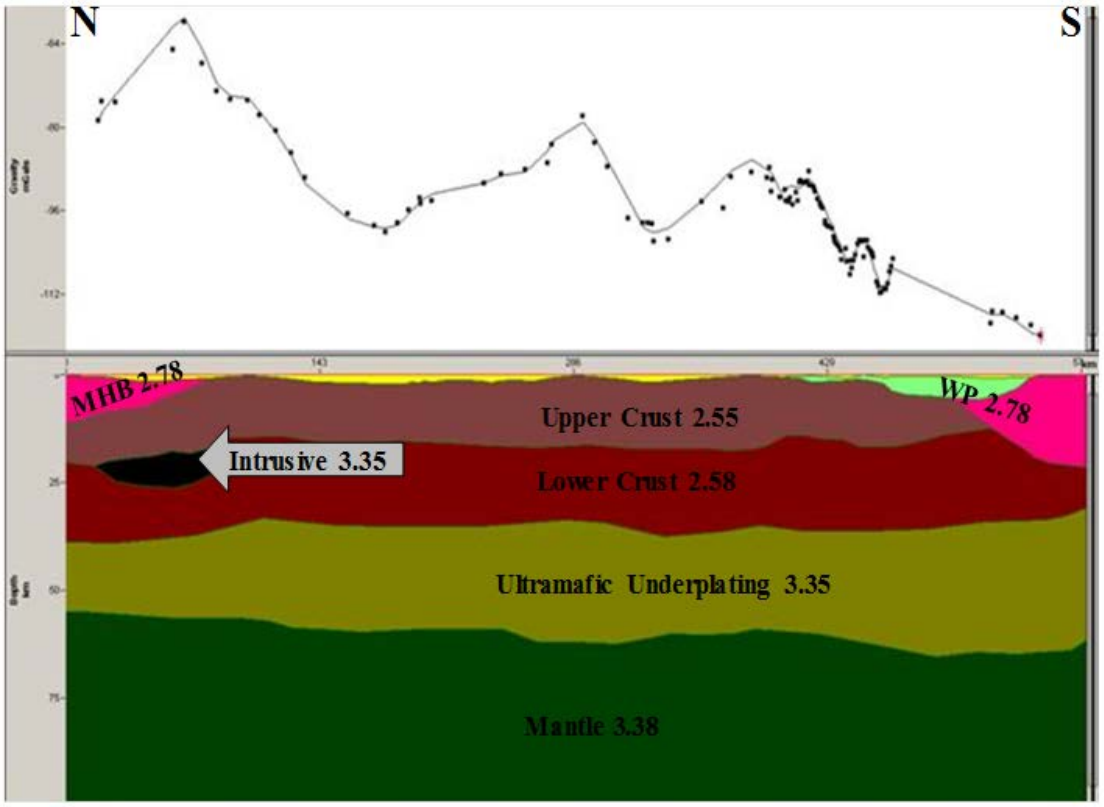

Figure 25. Gravity model along 108° longitude line. Solid line depicts calculated gravity value. Black dots represent actual gravity measured at a point during the study.

The gravity models provide a general crustal structure of the Wyoming Province in Montana. The most prominent feature is the underplated material that has been interpreted to possibly be remnant Proterozoic material emplaced during the subduction near the Wyoming Province (Gorman et al. 2000). The layer is thickest in the center of the Wyoming Province and thins toward the east next to the THO. In the east, the thicker upper crust layers may be related to a north dipping subduction zone. This may be related to accreted terranes from the south or the THO. With the absence of this thick layer to the west, the THO may be the cause of the crustal thickening.

5.20 Magnetotelluric Modeling

To interpret the MT data, 2-D inversion models were created. Two-dimensional models resulted in a cross sectional representation of the electrical resistivity variations. The data used to create the models were electrical impedance tensors that were decomposed into two separate modes; transverse magnetic (TM), and transverse electric (TE). The TM and TE modes can be represented by electrical resistivity and phases. The modeling program (WinGlink) inverts the TE and TM mode data to create an electrical resistivity cross section. The WinGlink software employs the Rodi and Mackie (2001) 2-D finite difference code to create two-dimensional models. The Rodi and Mackie (2001) code was used to perform the inversion for TM and TE mode resistivity at periods of 0.01s to 10,000s. The Rodi and Mackie code seeks a minimum structure 2-D resistivity model by beginning with a basic resistivity model that is modified through several iterations to produce a final resistivity model. Several models were produced using the TE, TM, and both modes, however only the best fit, TM mode results, will be discussed here as they are less affected by three-dimensional resistivity structures.
Figure 26 shows the geographical location of the three MT models.

The electrical resistivity structure for model 1 is shown in Figure 27. Resistivity values ranged from 29 ohms/m to 559 ohms/m. The higher resistive regions are interpreted to be Archean Provinces identified as the MHB on the northern edge of the model, and on the southern end is the Wyoming Province. The low resistivity zone roughly corresponds to the GFTZ which has been noted to the northeast in southern Alberta (Boerner et al. 1998). However, the thickness of the low resistivity zone extends to at least 300 km in depth beneath the MHB suggesting that there may be relic north-

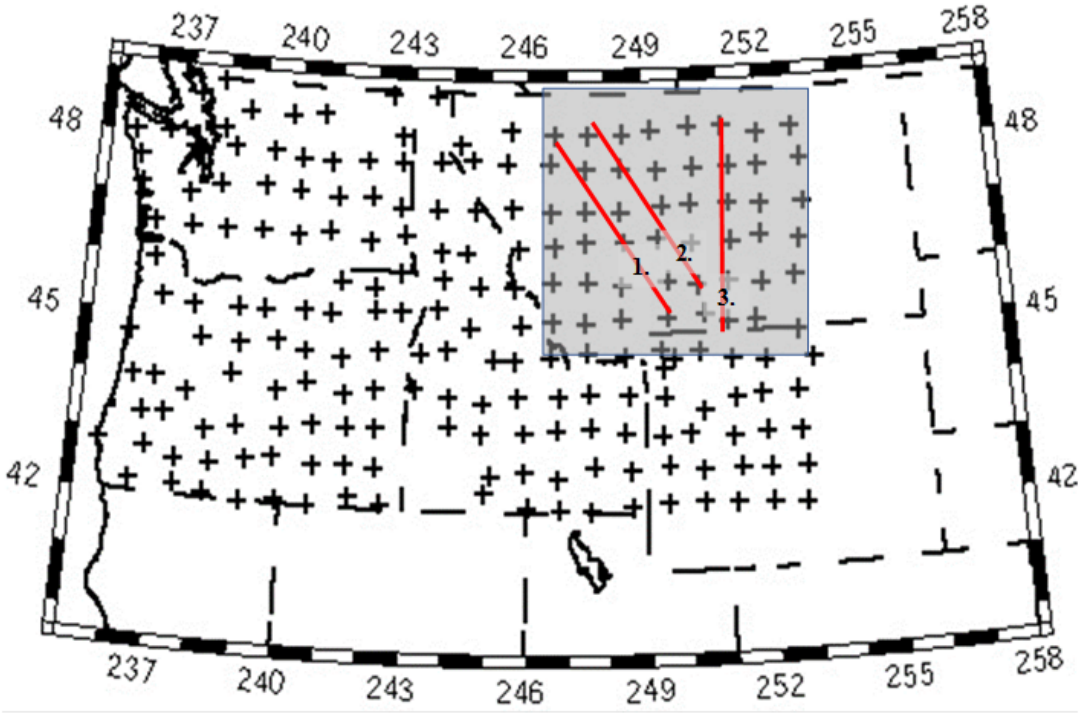

Figure 26. MT model locations of Earthscope transportable MT stations through 2009. The shaded area shows station locations used for this study. Red lines are MT model location profiels. Models are labeled 1, 2 and 3.

dipping subduction features beneath it. Also, note that the depth to the lithosphere-asthenospheric boundary (LAB) varies from 150 km beneath the MHB to 200 km beneath the Wyoming Province.

.

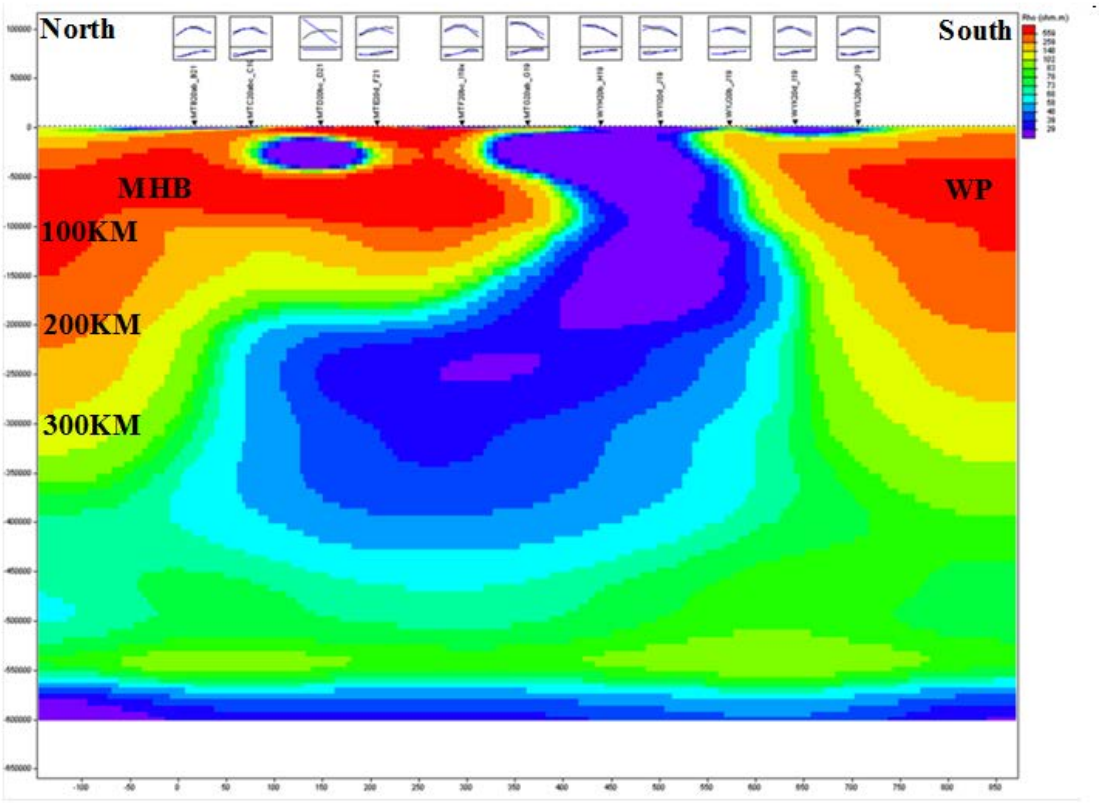

Figure 27. MT model 1. Final MT resistivity model along MT model 1. The letters n top of the model represent station location of the MT stations as seen in Figure 26. The curves above each station represent the calculated values (blue) and observed values (black). The top curves are apparent resistivities in ohms-m and the lower curves are phases in degrees. WP, Wyoming Province; MHB, Medicine Hat Block.

The electrical resistivity structure for model 2 is illustrated in Figure 28. Along this model, resistivity values range from 15 ohms/m to 375 ohms/m. The higher resistivity regions, similar to the model 1, portray the Archean Wyoming Province and Medicine Hat Block. This model does not indicate the north dipping remnant subduction like model 1. The depth to the LAB is 200 km under both the Wyoming Province and Medicine Hat Block.

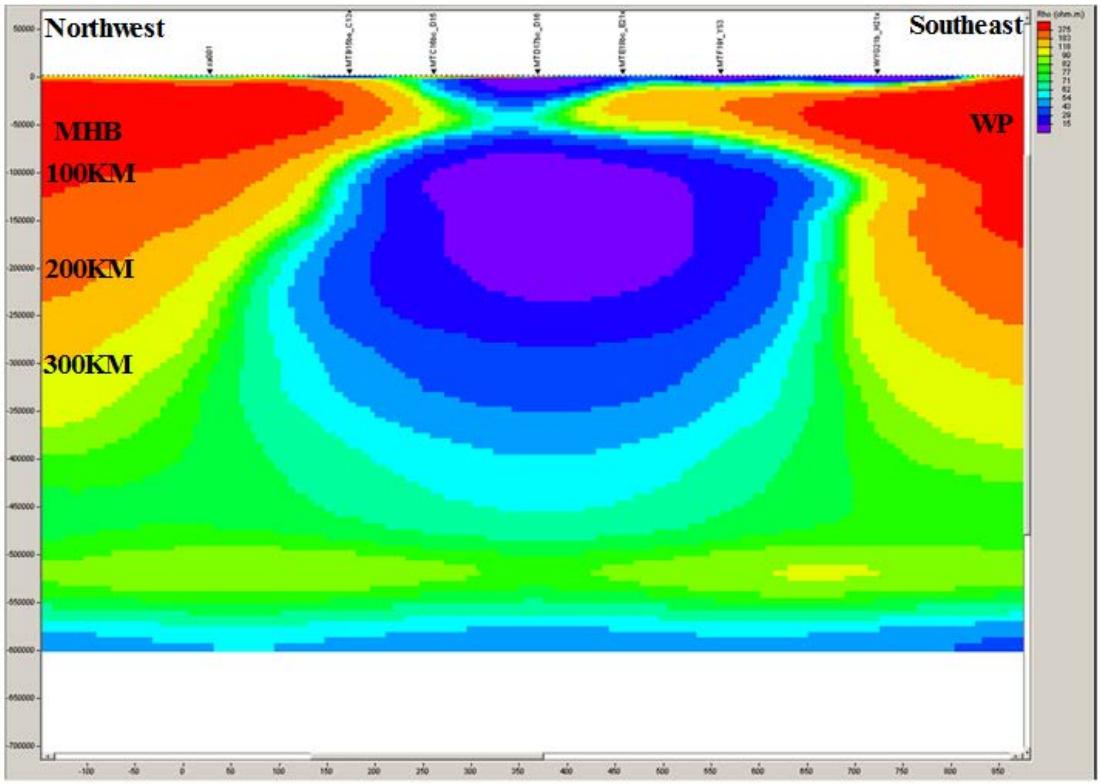

Figure 28. MT model 2. Final MT resistivity model along MT model 2. The letters along the top of the model represent the station location of the MT station locations as seen in Figure 26. MHB, Medicine Hat Block, WP. Wyoming Province.

The electrical structure for model 3, is shown in Figure 29. Resistivity values ranges from 11 ohms/m to 649 ohms/m. The low resistivity zone is south of the GFTZ implying that the structures forming the GFTZ may dip south or to the southeast. In contrast to model 1, the low resistivity zone dips toward the southeast beneath the WP. This low resistivity zone may be associated with the THO and agrees with the gravity model 3 which implies that the Wyoming Province in eastern Montana is influenced by the THO more than the implied north-dipping subduction in central Montana. Also, note

that the depth to the lithosphere-asthenospheric boundary (LAB) varies from 200 km beneath the Medicine Hat Block to 150 km beneath the Wyoming Province which is opposite than that found along model 1 in central Montana.

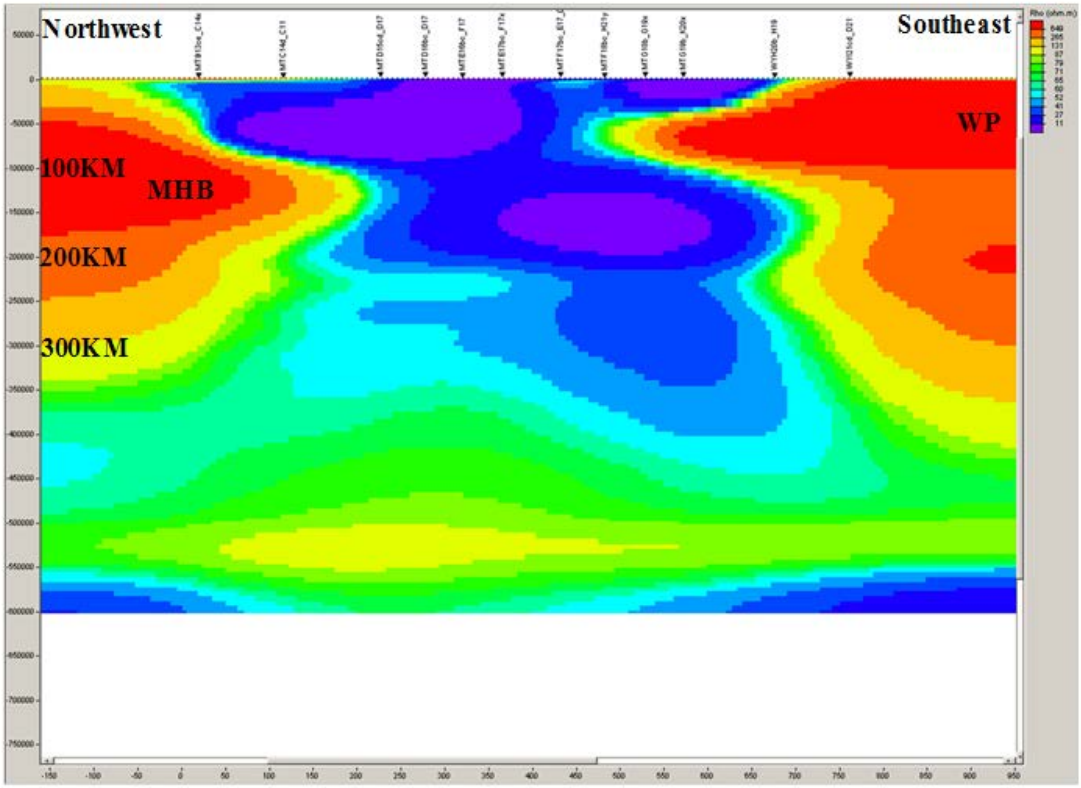

Figure 29. MT Model 3. Final MT resistivity model along MT model 3. The letters along the top of the model represent the location of the MT station locations as seen in Figure 26. MHB, Medicine Hat Block, WP, Wyoming Province.

5.30 Modeling Discussion

The MT models show the electrical resistivity structure of north central Montana. All the models ran for 100 iterations and show the approximate limits of resistivity sensitivity to be approximately 300 km. The most prominent feature of each model is the large highly conductive (low resistivity) region in the center of each model. This highly

conductive region extends downwards to approximately 200km or deeper. Within the continental crust there are multiple sources for enhanced resistivity. Possible causes for these anomalies may be the presence of aqueous fluids, partial melting, graphite, and/or metallic sulfides (Bedrosian and Box, 2016). Each of these are addressed below.

Aqueous Fluids. When considering aqueous fluids as an origin for enhanced resistivity three effects must be considered; the resistivity of the fluids, the distribution of the fluids, and the stability of the fluids. Resistivity is dependent upon temperature. Within partial melting regimes, temperatures can reach approximately 650°C (Bedrosian and Box, 2016). The source and stability of fluids at depth are also considerations. In active tectonic regimes, such as extensional environments, enhanced resistivity anomalies can be explained through aqueous fluids (Bedrosian and Box, 2016). Trace fluids can be consumed as rocks cool from equilibrium temperatures. However, in metamorphic environments the residence time for deep crustal water is ~100 million years. GFTZ is a compressional regime, not extensional and, based on our gravity and MT models, the region of north-central Montana has been compressional during the Precambrian. The slight possibility exists that the enhanced conductivity can be related to extensive Laramide deformation occurring 80 to 55 Ma.

Partial Melting. With respect to partial melting, enhanced resistivity anomalies will vary depending upon the distribution of the rocks' supporting matrix. Partial melting regions also exhibit lower seismic velocities and higher heat flow. However, Figure 5, shows that there was no decrease in seismic velocity within the vicinity of the enhanced resistivity region, thus partial melting is ruled out as an origin for the enhanced resistivity (Yardley and Valley, 1997; Clowes et al. 2002).

Graphite. Graphite is a highly conductive mineral that is commonly found in metasedimentary rocks (Yardley and Valley, 1997; Wannamaker, 2000). Graphite can be found anywhere within the crust, but is more abundant in the upper regions of the crust. Marine sediments commonly have high amounts of total organic carbon which convert to graphite during metamorphism. Metamorphic graphite is formed under extreme temperatures, >1000°C, unless strain energy is present (Bedrosian and Box, 2016).

If the GFTZ underwent transformation from a compressional boundary to a transpressional boundary as Mueller et al. (2002) suggest, strain energy was likely encountered during the suturing of the GFTZ to the WP and MHB, possibly distributing metamorphic graphite throughout the region. Metamorphic graphite is a possible explanation for the enhanced conductivity from just below the surface to 160km. The enhanced conductivity is within the graphite/diamond stability field range for graphite to exist, so it reasonable that graphite explains the upper enhanced conductivity anomalies within the models.

Metallic Sulfides. Similar to graphite, metallic sulfides can be a source of enhanced conductivity anomalies. Sulfides are found in sedimentary rocks where they are formed by the action of sulfate reducing bacteria, as in anoxic marine conditions (Bedrosian and Box, 2016). There is no evidence for the formation of sulfides within the GFTZ, therefore sulfides are not considered as the source for enhanced conductivity.

H^+ ions. The deeper seated conductive anomalies (>160km) need a different mechanism of emplacement. During episodes of subduction, water or minerals containing water are transported deeper into the mantle during which H^+ ions can become disassociated, creating free H^+ ions (Yardley and Valley, 1997; Bedrosian and Box,

2016). Previous studies have demonstrated that subduction occurred within the region of the GFTZ (Mueller et al. 2002). The deeper conductivity anomaly resides too deep to be explained by graphite, so it is possible the deeper lying conductive anomalies can be explained by the presence of free H^+ ions within the mantle.

6.0 CONCLUSIONS

The gravity and magnetic anomalies in central to eastern Montana and Wyoming reflect the combined effects of Archean to Paleoproterozoic to Cretaceous tectonic events. Transformation techniques such as bandpass filtering of the gravity and magnetic data were used to produce residual anomaly maps of Montana and Wyoming. The gravity field is dominated by crustal thickness variations with the thicker crust in Wyoming producing gravity minima. The residual gravity anomaly maps are dominated by gravity maxima which are related to Laramide Uplifts. However, the Great Falls Tectonic Zone is characterized by northeast-trending gravity maxima. The magnetic maps clearly defined the Wyoming Province in greater detail than the gravity anomaly maps. The Wyoming Province is seen by circular anomalies that coincide with the boundaries of the province. The Great Falls Tectonic Zone is also characterized by northeast-trending anomalies that are truncated by the north-south trending anomalies related to the Trans Hudson Orogeny

Two-dimensional gravity models constrained by regional seismic refraction models shows the of a lower crustal ultramafic underplated layer. The gravity models suggest that this layer exists only under the Wyoming Province and thins toward the east toward the Trans Hudson Orogeny.

The magnetotelluric analysis through the creation of three two-dimensional models revealed the existence of a region of low electrical resistivity between the Wyoming and the Medicine Hat Block Archean Provinces.

These lower resistivity anomalies are broken into upper and lower resistivity anomalies. The shallower (< 60 km) resistivity region can be explained by the presence of graphite within the metamorphic rocks. The deeper low resistivity region is deeper than the graphite/diamond stability field and may be caused by the dissolution of H+ ions within the mantle that was formed during Paleoproterozoic subduction.

Future work within the region should include the collection of additional magnetotelluric data and three-dimensional modeling of the magnetotelluric data, and creation of additional gravity models are needed to further understand the subsurface nature of the boundary interaction of the Wyoming Province and the GFTZ.

REFERENCES

Bankey, V., Cuevas, A., Daniels, D.L., Finn, C.A., Hernandes, I., Hill, P.L., Kucks, R.P., Miles, W., Pikington, M., Roberts, C., Roest, W.R., Rystrom, V.L., Shearer, S., Sweeny, R.E., Velez, J., Phillips, J.D., Ravat, D.K.A., 2002, Digital data grids for the magnetic anomaly map of the North America: Open-File Report, U.S. Geologic Survey.

Boerner, D.E., Craven, J.A., Kurtz, R.D., Ross, G.M., Jones, F.W., 1998, The Great Falls Tectonic Zone: suture or intracontinental shear zone: Canadian Journal of Earth Sciences, v. 35, p.175-183

Bedrosian, P. A., and S. E. Box., 2016, Highly conductive horizons in the Mesoproterozoic Belt-Purcell Basin: Sulfidic early basin strata as key markers of Cordilleran shortening and Eocene extension: Geological Society of America Special Papers, 522: 305-339.

Chamberlain, Kevin, R., Frost, Carol, D., Frost, B., Ronald, 2003, Early Archean to Mesoproterozoic evolution of the Wyoming Province: Archean origins to modern lithospheric architecture, v.40, p. 1357-1374

Clowes, Ron, M., Burianyk, Michael, J.A., Gorman, Andrew, R., Kanasewich, Ernest, R., Crustal velocity structure from SAREX, the Southern Alberta Refraction Experiment: Canadian Journal of Earth Sciences: v. 39, p. 351-373

Egbert, G.D., 1997. Robust multiple-station magnetotelluric data processing. Geophysical Journal International, v. 130(2), p.475-496.

Fedi, M., and Florio, G., 2001, Detection of potential fields source boundaries by enhanced horizontal derivative method: Geophysical Prospecting, v. 49, issue 1, p. 40-58.

Foster, David, A., Mueller, Paul, A., Mogk, David, W., Wooden, Joseph, L., Vogl, James, J., 2006, Proterozoic evolution of the western margin of the Wyoming craton: implications for the tectonic and magmatic evolution of the northern Rocky Mountains, Canadian Journal of Earth Sciences, v.43, p. 1601-1619

Frost, Carol, D., and Fanning, C., Mark, 2006, Archean geochronological framework of the Bighorn Mountains, Wyoming, Canadian Journal of Earth Sciences, v. 43, p. 1399-1418

Gorman, Andrew, R., Clowes, Ron, M., Ellis, Robert, M., Henstock, Timothy, J., Spence, George D., Keller, G., Randy, Levander, Alan, Snelson, Catherine, M., BUrianyk, Michael, J.A., Kanasewich, Ernest, R., Asudeh, Isa, Hajnal, Zoltan, Miller, Kate C., 2000, Deep Probe: imaging the roots of western North America: Canadian Journal of Earth Sciences, v. 39, p.375-398

Hammer, S., 1938, Investigation of the vertical gradient of gravity: Transactions-American Geophysical Union, v. 1, p. 71-82.

Hoffman, P.F., 1988. United plates of America, the birth of a craton: Early Proterozoic assembly and growth of Laurentia. Annual Review of Earth and Planetary Sciences, v. 16(1), pp.543-603.

Iyer, H.M., Pakiser, L.C., Stuart, D.J. and Warren, D., 1969. Project Early Rise: seismic probing of the upper mantle. Journal of Geophysical Research, v. 74(17), pp.4409-4441.

Jones, A.G., Ledo, J. and Craven, J.C., 2003, April. Electrical parameter maps of Canada derived from Lithoprobe surveys. In EGS-AGU-EUG Joint Assembly.

Jones, A.G., Lezaeta, P., Ferguson, I.J., Chave, A.D., Evans, R.L., Garcia, X. and Spratt, J., 2003. The electrical structure of the Slave craton. Lithos, v. 71(2), pp.505-527.

Leeman, W.P., 1982. Development of the Snake River Plain-Yellowstone Plateau province, Idaho and Wyoming: an overview and petrologic model. Cenozoic geology of Idaho: Idaho Bureau of Mines and Geology Bulletin, v. 26, pp.155-177.

Meqbel, N.M., Egbert, G.D. and Kelbert, A., 2011, Three dimensional electrical conductivity model of the Northwestern US derived from 3-D inversion of USArray magnetotelluric data: In AGU Fall Meeting Abstracts, Vol. 1, p. 2093.

Mickus, K., 2007, Precambrian blocks and orogen boundaries in the north-central United States determined from gravity and magnetic data: in Hatcher, R., Carlson, M., McBride, J., and Martinez J., eds ,4-D Framework of Continental Crust: Geological Society of America Memoir 200, p. 327-340.

Mueller, P., A., and Frost, C.D., 2006, The Wyoming Province: a distinctive Archean craton on Laurentian North America: Canadian Journal of earth Sciences, v. 43, p.1391-1397

Mueller, P.A., Heatherington, A.L., Kelly, D.M., Wooden, J.L. and Mogk, D.W., 2002. Paleoproterozoic crust within the Great Falls tectonic zone: Implications for the assembly of southern Laurentia. Geology, v.30(2), pp.127-130.

Mueller, Paul A., and Wooden, Joseph, L., 1988, Evidence for Archean subduction and crustal recycling, Wyoming province: Geology, v. 16, p.871-874

Mueller, P.A., Wooden, J.L., Mogk, D.W., Henry, D.J. and Bowes, D.R., 2010. Rapid growth of an Archean continent by arc magmatism. Precambrian Research, v. 183(1), pp.70-88.

Nagy, D., 1966, The prism method for terrain corrections using digital computers: Pure and Applied Geophysics, v. 63, p. 31-39.

Németh, B. and Hajnal, Z., 1998. Structure of the lithospheric mantle beneath the Trans-Hudson Orogen, Canada. Tectonophysics, 288(1-4), pp.93-104.

Reynolds, J.M., 1997. An introduction to applied and environmental geophysics: West Sussex. Wiley & Sons: Chichester, United Kingdom, p. 796.

Sears, J.W., 2007, Rift destabilization of a Proterozoic epicontinental pediment: A model for the Belt-Purcell basin, North America, in Proterozoic Geology of Western North America and Siberia, Link, P.K., and Lewis, R.S., eds.: SEPM Special Publication, 86, p. 55-64.

Thybo, H. and Perchuć, E., 1997. The seismic 8 discontinuity and partial melting in continental mantle. Science, v. 275(5306), pp.1626-1629.

Yardley, Bruce W.D. and Valley, John W., 1997, The petrologic case for a dry lower crust: Journal of Geophysical Research, v. 102, NO B6, p. 12,173-12,185

Wannamaker, Phillip, E., 2000, Comment on "The petrologic case for a dry lower crust" by Bruce W.D. Yardley and John W. Valley, Journal of Geophysical Research, v. 105, NO B3, p. 6057-6064

Whitmeyer, Steven, J., and Karlstrom, Karl, E.,2007, Tectonic model for the Proterozoic growth of North America: Geosphere, v. 3, p. 220-259

Winston, D., and Sears, J.W., 2013, Stratigraphy of the Proterozoic Belt Supergroup and structure of the Belt Basin: Glacier National Park, in Lewis, R.S., Garsjo, M.M., and Gibson, R.I., eds., Belt Symposium V, Northwest Geology, v. 42, p. 237-256.